corrosion and materials degradation

MDPI

Article

Microbial Communities in Model Seawater-Compensated Fuel Ballast Tanks: Biodegradation and Biocorrosion Stimulated by Marine Sediments

Kathleen E. Duncan [1,*], Lina E. Dominici [2,*], Mark A. Nanny [3], Irene A. Davidova [1], Brian H. Harriman [1,4] and Joseph M. Suflita [1]

[1] Department of Microbiology & Plant Biology, University of Oklahoma, Norman, OK 73019, USA; davidova@ou.edu (I.A.D.); bharriman@lanl.gov (B.H.H.); jsuflita@ou.edu (J.M.S.)
[2] Centro de Investigación y Desarrollo en Tecnología de Pinturas (CIDEPINT), CICPBA-CONICET-UNLP, La Plata B1900AYB, Argentina
[3] School of Civil Engineering and Environmental Science, University of Oklahoma, Norman, OK 73019, USA; nanny@ou.edu
[4] Bioscience Division, Los Alamos National Laboratory, Los Alamos, NM 87544, USA
* Correspondence: kathleen.e.duncan-1@ou.edu (K.E.D.); l.dominici@cidepint.ing.unlp.edu.ar (L.E.D.)

Abstract: Some naval vessels add seawater to carbon steel fuel ballast tanks to maintain stability during fuel consumption. Marine sediments often contaminate ballast tank fluids and have been implicated in stimulating fuel biodegradation and enhancing biocorrosion. The impact of the marine sediment was evaluated in model ballast tank reactors containing seawater, fuel (petroleum-F76, Fischer–Tropsch F76, or a 1:1 mixture), and carbon steel coupons. Control reactors did not receive fuel. The marine sediment was added to the reactors after 400 days and incubated for another year. Sediment addition produced higher estimated bacterial numbers and enhanced sulfate reduction. Ferrous sulfides were detected on all coupons, but pitting corrosion was only identified on coupons exposed to FT-F76. Aerobic hydrocarbon-degrading bacteria increased, and the level of dissolved iron decreased, consistent with the stimulation of aerobic hydrocarbon degradation by iron. We propose that sediments provide an inoculum of hydrocarbon-degrading microbes that are stimulated by dissolved iron released during steel corrosion. Hydrocarbon degradation provides intermediates for use by sulfate-reducing bacteria and reduces the level of fuel components inhibitory to anaerobic bacteria. The synergistic effect of dissolved iron produced by corrosion, biodegradable fuels, and iron-stimulated hydrocarbon-degrading microbes is a poorly recognized but potentially significant biocorrosion mechanism.

Keywords: marine sediments; ballast tank; biocorrosion; microbiologically influenced corrosion; sulfate-reducing bacteria; petroleum F76 fuel; Fischer–Tropsch F76 fuel; fuel biodegradation; aerobic hydrocarbon degradation; iron stimulation

Citation: Duncan, K.E.; Dominici, L.E.; Nanny, M.A.; Davidova, I.A.; Harriman, B.H.; Suflita, J.M. Microbial Communities in Model Seawater-Compensated Fuel Ballast Tanks: Biodegradation and Biocorrosion Stimulated by Marine Sediments. *Corros. Mater. Degrad.* **2024**, *5*, 1–26. https://doi.org/10.3390/cmd5010001

Academic Editor: Daniel John Blackwood

Received: 2 November 2023
Revised: 18 December 2023
Accepted: 22 December 2023
Published: 3 January 2024

1. Introduction

The microbial ecology of ship ballast tanks is important because the associated solids and fluids may transport invasive and/or pathogenic organisms [1–4] and constitute microbial communities that can enhance fuel decay and metal corrosion [5–7]. Marine sediments accumulate in ship ballast compartments together with corrosion products from the machinery used to manage water intake and output. Collectively, these solid phases form a ballast tank sediment or sludge [1,5,8,9]. The entrainment and accumulation of marine sediment in ballast tanks is common, particularly when a vessel takes on ballast water in relatively shallow areas [5,10]. Indeed, the realization that ballast water exchange in polluted harbor waters with its associated high nutrient load and sediment may promote microbially influenced corrosion (MIC) has led to the recommendation that such exchanges take place well offshore [5].

Although marine sediments are a major source of microorganisms in ballast tanks, the associated solids are expected to harbor a somewhat distinct microbial assemblage [4,11,12] since ballast tanks have a generally greater concentration of metals and disinfection byproducts [6,8,9]. Consequently, the ballast tanks constitute environmental compartments suitable for the proliferation of many types of microbes, including biocorrosive microorganisms [7–9,13]. Fuel-compensated ballast tanks typically use both fuel and seawater for the ballast and, therefore, may be particularly susceptible to MIC, as the petroleum distillate represents a near-continuous source of carbon and energy for hydrocarbon-degrading microbes [5,14–17]. An initial field study investigated microbial succession patterns and metal biocorrosion in naval vessels with fuel-compensated ballast tanks [7]. Ballast water samples from ships that had been recently replenished showed a marked increase in the relative abundance of aerobic hydrocarbon-degrading Gammaproteobacteria compared to the harbor seawater. Ballast water that had a shipboard residence time in months contained microbial communities dominated by Deltaproteobacteria, primarily sulfate-reducing bacteria (SRB), and evidence for anaerobic hydrocarbon biodegradation processes, including requisite genes and their associated metabolites. These findings suggest a successional process initially favoring first aerobic hydrocarbon-degrading bacteria followed by anaerobic hydrocarbon-degrading organisms as oxygen consumption exceeded the resupply. Metal biocorrosion was also implicated by the elevated levels of Fe, Mn, Ni, and Cu in the ballast tank samples [7,9].

In a follow-up laboratory study [18], using a seawater inoculum, we monitored ballast tank model reactors that contained carbon steel coupons and two types of F76 diesel fuel: either a traditional petroleum marine diesel fuel [19], e.g., petro-F76, an alternative marine diesel produced through the Fischer–Tropsch process (FT-F76), or a 1:1 mixture of the two fuels. Although the commercialization of Fischer–Tropsch fuels date back to the 1930s [20], questions remain about their suitability when stored with seawater [19]. The two fuels differ in their chemical composition, with FT-F76 containing a much lower proportion of aromatic and polyaromatic compounds than petro-F76 but a higher proportion of isoalkanes [19,21]. Such differences in chemical composition are expected to affect the biodegradability of the fuel [22,23] and the composition of the hydrocarbon-degrading microbial community. In turn, differences in community composition may influence the rate and degree of biocorrosion.

It is known that many types of bacterial physiology can be part of a microbial community associated with corroding metals. However, the mere presence of these microbes, while suggestive, does not sufficiently implicate them in corrosion processes [24,25]. The use of multiple lines of evidence is strongly recommended [25–28]. The evidence for this can include measures of microbial activity [29] in combination with an analysis of diagnostic chemicals and environmental parameters, as well as the mineralogy of corrosion products [30–32] and electrochemical measurements [33], which help bolster the case for metal corrosion. Some corrosion products are associated with microbes, such as FeS (mackinawite) with sulfate-reducing bacteria [34], magnetite (Fe_3O_4) with dissimilatory Fe(III)-reducing bacteria [35], and two-line ferrihydrite with iron-oxidizing bacteria [27,35]. The above notwithstanding, some mineral phases can be formed abiotically [27] and undergo transformations over time in response to abiotic [30,31,36] and biotic factors [37,38]. Given this degree of complexity, it can be difficult to unambiguously attribute specific corrosion minerals to different biotic processes.

Given these considerations, multiple lines of investigation were collected to examine the relationship between the biodegradation of the two diesel fuels and carbon steel biocorrosion in model fuel-compensated ballast tanks. We showed that the petro-F76-amended seawater reactors developed different microbial community compositions, open circuit potential (OCP), pH and dissolved iron levels than reactors amended with FT-F76 fuel. However, contrary to the results from samples taken from shipboard fuel-compensated ballast tanks [7], the model reactors exhibited a poor sulfate reduction activity, even though sulfate levels were replete and SRBs constituted a substantive portion of the resident mi-

croflora. A low rate of oxygen diffusion across the polycarbonate housing the reactors was hypothesized as a reason for the limited sulfate reduction activity and the possible promotion of sulfide oxidation [39–42] consistent with the detection of a high relative abundance of sulfide-oxidizing bacteria in two of the reactors [18]. The relatively low levels of sulfate reduction and dissolved iron suggested that the rate of corrosion was relatively slow. Furthermore, the low relative abundance of hydrocarbon-degrading bacteria suggested that the fuel-amended seawater reactors did not have conditions that were particularly conducive to fuel biodegradation. A component not included in the Dominici et al. [18] study was the inclusion of a marine sediment. In another laboratory study of biocorrosion using a variety of naval fuels, carbon steel coupons, and marine inocula [21], the degree of both general and pitting corrosion was positively correlated with the loss of the sulfate, implicating sulfate-reducing bacteria as major contributors to MIC. However, the rate of sulfate loss and extent of corrosion varied with the inoculum, and both were more extensive when marine sediments were incorporated into the experiment.

In this study, the model reactors were amended with marine sediments from the same harbor that seawater was obtained from in order to examine the effect of the added solid phase and associated microflora on sulfate reduction, hydrocarbon degradation, and carbon steel corrosion. The addition of sediment, especially sediments containing live microbiota, produced higher estimated bacterial numbers, an increase in the relative abundance of hydrocarbon-degrading bacteria, and enhanced sulfate reduction. Generalized corrosion was detected for both types of fuel. Pits were seen only on coupons from reactors amended with FT-F76. Reactors before sediment addition contained high levels of dissolved iron and showed a decrease in the level of dissolved iron after the addition of the sediment, together with an increase in the relative abundance of aerobic hydrocarbon-degrading bacteria. Previous studies noted that dissolved iron stimulates aerobic hydrocarbon-degradation activity [43,44]. Other research has shown how the production of intermediates of aerobic fuel biodegradation help provide suitable electron donors for biocorrosive anaerobic communities [45], while other studies implicated aerobic hydrocarbon-degrading bacteria in the promotion of MIC [46]. Other studies suggest that decreasing inhibitory fuel components through biodegradation may differentially facilitate anaerobic activities associated with MIC [47,48].

Thus, we propose that marine sediments added to a ballast tank containing seawater and biodegradable fuel, especially when corrosion has produced some dissolved iron, ultimately stimulate MIC through the activity of aerobic hydrocarbon-degrading microbes. Their activities provide electron donors and other nutrients for anaerobic bacteria and reduce the level of inhibitory fuel components and oxygen. Anaerobic hydrocarbon degradation and MIC are then expected to dominate as successional processes as conditions become more favorable for anaerobic microbial assemblages. Triggered by the addition of marine sediments and a transitory increase in oxygen levels, the interaction of susceptible metal, the dissolved iron produced during initial corrosion events, iron-stimulated hydrocarbon-degrading microbes, and biodegradable fuels could produce a positive MIC feedback cycle.

2. Materials and Methods

2.1. Reactor Design

Duplicate reactors containing 24 coupons (1018 carbon steel, Metal Samples, Munford, AL measuring 1.3 cm × 7.6 cm × 0.15 cm) were inoculated with approximately 2550 mL of seawater from San Diego Bay Harbor (San Diego, CA, USA) and a total of 120 mL of either petro- or Fischer–Tropsch F76 (FT-F76) fuel or a 50:50 mix of both fuels (Figure 1 and Table 1) and were incubated for 400 days. Note that approximately 6×10^{-6} moles of oxygen were diffused into a reactor per day [49] based on the oxygen permeability properties of the polycarbonate used in the construction of the reactor [18].

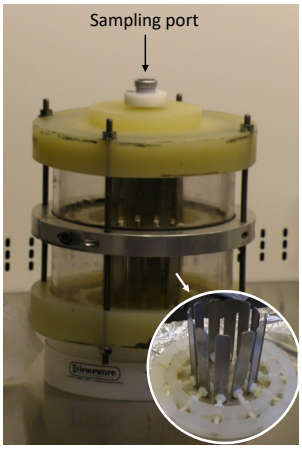

Figure 1. Rotating ballast tank reactors [18]. An assembled reactor with 2 holders of coupons (24 coupons total). The reactors were filled with seawater from San Diego Bay. The holder with 1018 carbon steel coupons is shown in the inset photo.

Table 1. Reactor composition and experimental design. Fuel and seawater were added at the start of the experiment, and the sediment was added on day 400 (start of phase 2). The added sediment was either heated-treated by autoclaving (HT) or was untreated and therefore nonsterile (NS). See Section 2.1 for more information.

Reactor	Fuel Type	Sediment Treatment
R1	Petro-F76	NS
R2	Petro-F76	HT
R3	FT-F76	NS
R4	FT-F76	HT
R5	Petro- and FT-F76	NS
R6	Petro- and FT-F76	HT
R7	No fuel	NS
R8	No fuel	HT

After 400 days, reactors were placed in a glove bag under an N_2 atmosphere to obtain the final phase 1 samples, and sediment was added to initiate phase 2. One replicate of each treatment received either heat-sterilized (autoclaved at 121 °C for 20 min, [50]) or untreated nonsterile sediments consisting of a slurry of 100 mL of seawater and a 100 g (wet weight) sediment. Sediment slurries were flushed with N_2:CO_2 (80:20) gas for oxygen removal. The slurries were added through sterile funnels. The operation of the reactors was divided into two phases. Phase 1 consisted of the study of the reactors from day 0 to 400, as reported previously [18], and phase 2 from day 400 to day 764, as described here. The samples were taken through the sampling port with a syringe flushed with N_2.

2.2. Chemical Analyses

Dissolved sulfide was measured immediately after sample collection using the methylene blue method (Sulfide VACUettes kit K-9510D, CHEMetrics, Midland, VA, USA). The sulfate was quantified by ion chromatography as previously described [18,50]. Dissolved metal concentrations were measured as previously described after filtering the sample through a 0.45 µm PES filter (Whatman Puradisc, Sigma-Aldrich, St. Louis, MO, USA) [7,18].

The open circuit potential (OCP) and pH were measured in a 10 mL subsample transferred to a small crimp-sealed electrochemical cell using a syringe flushed with N_2 gas. All OCP and pH measurements were made inside an anaerobic chamber with a 95% N_2 and 5% H_2 gaseous atmosphere. The open circuit potential was measured with an Ag/AgCl reference electrode and a platinum measurement electrode [51]. All OCP data in the text,

figures, and graphs are presented as values referenced to a standard hydrogen electrode (SHE). The pH measurements were obtained with an Orion 350 pH meter and Oakton pH electrodes. A three-point calibration curve, using pH buffer standards at pH = 4, 7, and 10, was used for each measurement.

2.3. Scanning Electron Microscopy (SEM) and Energy Dispersive X-ray (EDX) Methodology

Coupons were removed at the conclusion of the experiment from the reactors in an anaerobic chamber and placed in a sealed container with an inert atmosphere (5% H_2 and 95% N_2) until they were transferred to the SEM-EDS chamber to ensure that the time of atmospheric exposure was less than 2 min. SEM was performed using a Zeiss NEON 40 EsB (Carl Zeiss, Oberkochen, Germany) scanning electron microscope and EDX was performed using an OXFORD Link Pentafet X-ray analyzer with IXRF software (Spirit V. 1.07.05). The images were obtained under 1000 kX magnification using an acceleration voltage of 15 kV and a working distance of 9 mm. The entire surface of the sample was examined under low magnification (300 kX). The selected typical area was examined with EDX under 1000 kX magnification and each EDX scanning area was 1 μm × 1 μm. Two scan areas per coupon were examined with 4 to 7 points (individual spectra) scanned per area (Table S2). In total, 8 to 14 spectra were obtained for each coupon.

2.4. Sulfate Reduction Assay

The rates of sulfate reduction in triplicate samples were measured using a previously described radiotracer technique [18,29]. The bottles were incubated for 7–8 days at room temperature (about 21 °C). The amount of ^{35}S in an aliquot of the trap solution was quantified via scintillation counting.

2.5. Sample Collection and DNA Extraction

Duplicate 20 mL samples of a 1:1 mix of the San Diego Bay seawater/sediment were used to inoculate the reactors and filtered through 0.2 μm pore size PES filters (cat # 567-0020, ThermoScientific, Carlsbad, CA, USA,). The filters were then placed in 50 mL sterile Falcon tubes with 1 mL of DNAzol (DN127, Molecular Research Center, Inc., Cincinnati, OH, USA) and were stored at −80 °C until DNA was extracted. Fluid samples from the reactors were collected at the end of experiment day 764 (700–900 mL). Reactor fluid samples were preserved for DNA extraction by first filtering through a 0.2 μm pore size PES filter (ThermoScientific cat # 567-0020). The filters were then placed in 50 mL sterile Falcon tubes with 1 mL of DNAzol (DN127, Molecular Research Center, Inc., Cincinnati, OH, USA) and were stored at −80 °C until DNA was extracted.

DNA extraction from the filtered samples was performed as described previously [18] with beadbeating followed by extraction using the Maxwell® 16 Tissue LEV Total RNA purification kit (Promega, Madison, WI, USA). The coupon and sediment samples were collected at the end of the experiment in 50 mL sterile Falcon tubes containing 1 mL of DNAzol. The coupons were rinsed on each side several times with the contained DNAzol and stored at −80 °C prior to DNA extraction. Sediments were vortexed to thoroughly mix with the DNAzol and stored at −80 °C. The biofilm on the coupons was removed with autoclaved Teflon tissue culture scrapers (#50-197-8422 ThermoFisher Scientific). DNA from the coupons and sediment (~0.5 g aliquots) was extracted using a PowerSoil DNA Isolation Kit (MoBio Laboratories, Carlsbad, CA, USA) following the manufacturer's instructions. Some coupon samples, due to the presence of PCR inhibitors, were pretreated before the Powersoil extraction via the addition of 100 μL of CTAB/NaCl (10% hexadecyltrimethyl ammonium bromide, 4.1% NaCl, JGI Bacterial DNA Isolation CTAB Protocol) and incubated at 70 °C for 10 min.

2.6. Quantification of 16S rRNA by Quantitative PCR

The total number of bacterial and archaeal 16S rRNA gene copies was estimated using the primers S-D-Arch-0519-a-S-15 and S-D-Bact-0785-b-A-18 [52]. Thermal cycling, data

acquisition, and analyses were carried out with the StepOnePlus™ Real-Time PCR System and StepOne Software v2.1 (Life Technologies, Carlsbad, CA, USA), following the protocol previously described [18]. For each qPCR run, a 1:10 dilution series of a control DNA plasmid containing a bacterial 16S rRNA gene sequence was used to generate a 7-point standard curve. Standards, no-template controls, and samples were assayed in triplicate.

2.7. Construction and Analysis of 16S rRNA Amplicon Libraries

An aliquot of DNA extracted from the samples was used to generate 16S amplicon libraries with distinctive barcodes as previously described [18,53].

Briefly, the M13-519F/785R primer set (specifically primers S-D-Arch-0519-a-S-15 and S-D-Bact-0785-b-A-18, [52]) was used to amplify the V3–V5 region of the 16S rRNA gene, and a 12 base pair sequence conjugated to M13 [54] was used to barcode each sample. All amplicon library sequences were deposited in the NCBI Sequence Read Archive under Bioproject accession number PRJNA875099.

Amplicon library sequences were processed using the open-source package DADA2 (Divisive Amplicon Denoising Algorithm) in R software version 4.2.1 [55,56]. Amplicon sequence variants (ASV) were inferred, and taxonomic affiliations were determined using the SILVA v132 database as the reference database. Microbial community analysis was performed on the rarefied samples to 3338 sequences using R package Alpha diversity indices and was calculated based on the Hill number [57] using the HillR package. The number of reads and alpha diversity measurements are summarized in Table S1. Beta diversity analysis was performed using the principal coordinate analysis (PCoA) biplot based on the Unifrac weighted distance matrix using phyloseq and ggplot2 packages [58].

2.8. Statistical Analysis

One-way ANOVA with Tukey's honestly significant difference (2-sided) post hoc test was used to analyze the microbial community composition data at the genus level using the Statistical Package for the Social Sciences (SPSS for Windows version 28.0.0, IBM, Chicago, IL, USA). The significance level was set at 0.05.

3. Results

3.1. Chemical Analyses

3.1.1. OCP and pH

The OCP and pH were monitored throughout the experiment to track bulk redox conditions and changes in pH that might indicate microbial activity (Figure S1, phase 2). Note that approximately 6×10^{-6} moles of oxygen were diffused into a reactor per day [49] due to polycarbonate reactor housing. Immediately prior to sediment addition, samples from the reactors formed two groups (Figure 2a). Group 1 reactors containing either the petro fuel (R1, R2) or the 50:50 mix (R5, R6) with OCP values of −300 to −325 mV and pH values between 7.5 and 7.8. Group 2 consisted of the reactors with FT-F76 fuel (R3, R4) and one of the no-fuel reactors (R8) with OCP values between −200 and −250 mV and a pH between 8.1 and 8.4. The other no-fuel reactor had a higher OCP (−95 mV) and pH of 8.3.

After the addition of the sediment (phase 2), all reactors experienced substantive changes in OCP and pH for more than a month, with more gradual changes occurring for at least 100 days thereafter (Figure S1). After approximately 325 days post sediment addition, most reactors were labeled as Group 4 with higher, but still negative, OCP values (−35 to −100 mV) and higher pH (8.3 to 8.5, Figure 2b) values. The fuel-containing reactors receiving the heat-treated sediment (R2 and R6) formed Group 3, with a lower pH than any other reactor and a slightly lower OCP than the Group 4 reactors. It was clear that the phase 2 reactors represented a weaker reducing environment than prior to sediment addition (phase 1; [18]).

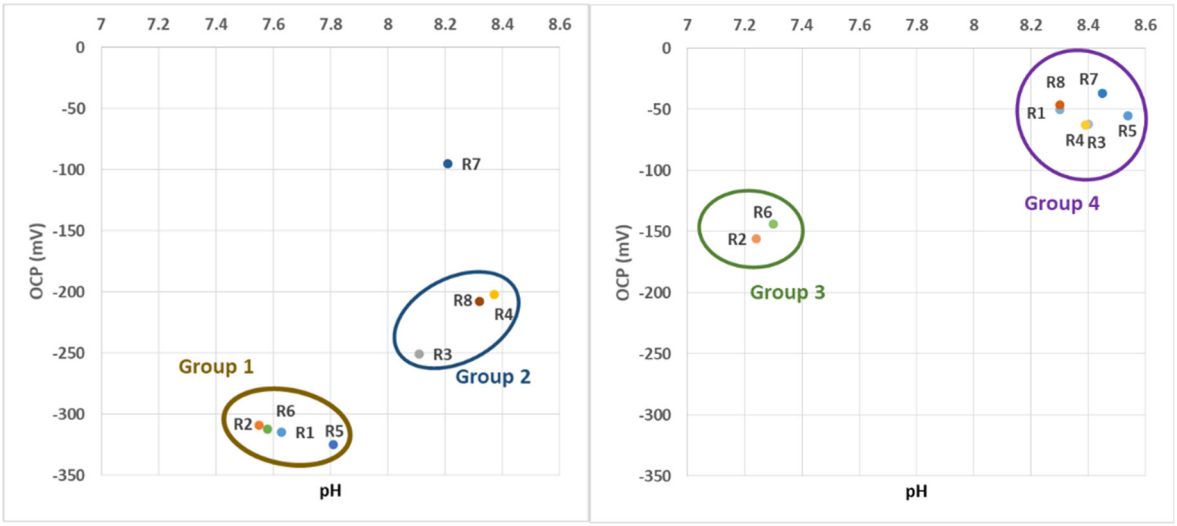

Figure 2. Open-circuit potential (OCP) and pH values of phase 1 and 2 liquid samples. The bivariate plot of pH versus open-circuit potential (OCP, mV). OCP values are referenced to a standard hydrogen electrode (SHE). R1, R2: petro F76 fuel. R3, R4: FT-F76 fuel. R5, R6: mix of petro- and FT-F76 fuel. R7, R8: no fuel added. (**a**) Phase 1, samples collected on day 400, before sediment addition. (**b**) Phase 2, samples collected on day 750, approximately 350 days post sediment addition. Nonsterile sediments were added to R1, R3, R5, R7; autoclaved sediments were added to R2, R4, R6, R8.

3.1.2. Sulfur Species

Changes in the fluid-phase sulfate concentration were monitored by ion chromatography, while the rate of sulfate reduction was assessed with a radioactive tracer. All reactors except R2 and R6 had lower levels of sulfate than the initial seawater concentration (28.1 mM) by the end of phase 1. The addition of the sediment and fresh seawater during the start of phase 2 resulted in sulfate concentrations approaching that of seawater. This level of sulfate persisted for approximately 2 months (up to day 458) in all reactors containing fuel. Afterward, the reactors that received sediment with live microbiota (R1, R3, R5, R7), and also R4, saw a decrease of 2 mM or more in sulfate levels, while the levels in R2, R6, and R8 did not decrease until the final sampling.

The rates of sulfate reduction were significantly above the background (0.032 µmol S/mL/day) on two occasions after sediment addition (Figure 3: red stars, Table S3A), once for R6 (fuel mix) and once for R4 (FT-F76). Dissolved H_2S was never detected during phase 1 but was first detected about a month after sediment addition (Figure 3: red circles Table S3B). Dissolved H_2S was detected repeatedly in reactors R3, R4 (FT-F76), and R6 (fuel mix), less often in R7 and R8 (no fuel) and once in R2 (petro-F76) and R5 (fuel mix). Dissolved H_2S levels were never above 7.5 ppm.

3.1.3. Dissolved Fe

The dissolved Fe concentration in the harbor seawater used in the reactors was 16.2 ppb. Prior to sediment addition, increased dissolved Fe concentrations (Figure 4) were related to lower pH and OCP values (Figure 2a, Group 1, R1, R2, R5, R6), which is consistent with the prospect that the pH and OCP control the iron speciation between soluble Fe^{2+} and insoluble ferric oxides.

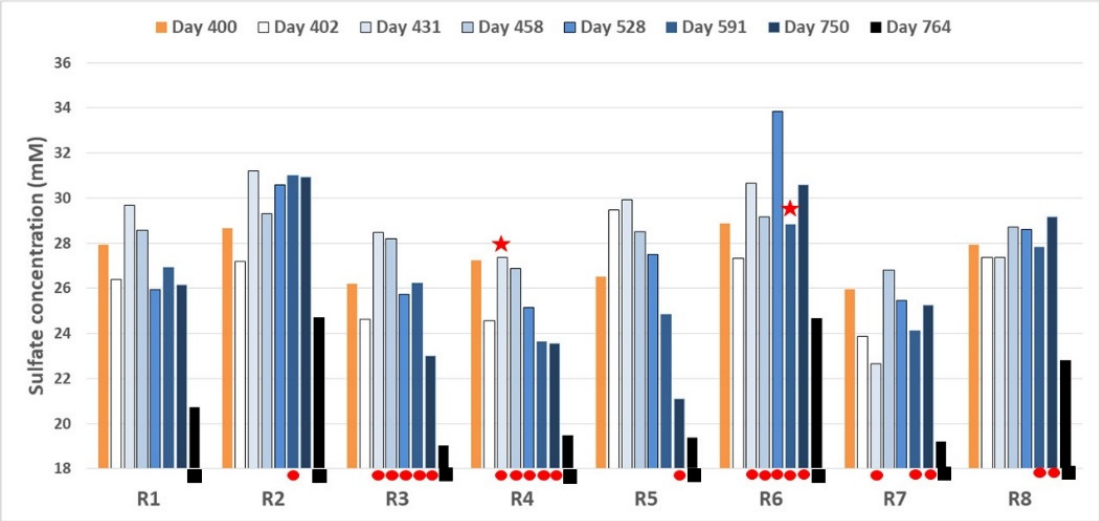

Figure 3. Sulfate concentrations (mM). Orange bars: sulfate concentration before sediment addition (day 400). Blue bars: sulfate concentration after sediment addition. Red circles: H_2S detected. Black boxes: H_2S not sampled on this date. Red stars: significant rates of sulfate reduction. R1, R2: petro-F76 fuel. R3, R4: FT-F76 fuel. R5, R6: mix of petro- and FT-F76 fuel. R7, R8: no fuel added. Nonsterile sediments were added to R1, R3, R5, R7; autoclaved sediments were added to R2, R4, R6, R8.

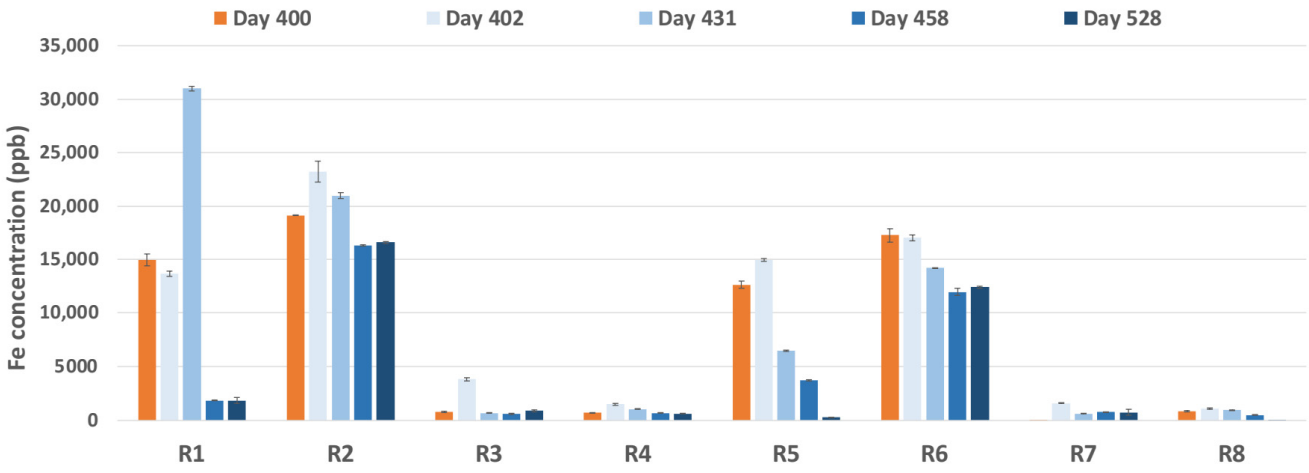

Figure 4. Dissolved iron concentration. Orange bars: iron concentration before sediment addition (day 400). Blue bars: iron concentration after sediment addition. R1, R2: petro-F76 fuel. R3, R4: FT-F76 fuel. R5, R6: mix of petro- and FT-F76 fuel. R7, R8: no fuel added. Error bars indicate ± 1 standard deviation. Nonsterile sediments were added to R1, R3, R5, R7; autoclaved sediments were added to R2, R4, R6, R8.

For R1 and R5, the addition of the sediment with live microbiota caused the dissolved iron concentration to decrease to barely measurable values after about 100 days, while the addition of the heat-treated sediment to the reactors R2 and R6 did not dramatically change the dissolved iron concentration during this period. Concurrently, Figure 3 shows that reactors R1 and R5 experienced sulfate loss, while R2 and R6 did not show a loss of the sulfate until day 764. This indicates that sulfate reduction was occurring and driving the formation of iron sulfides earlier in R1 and R5 than in R2 and R6. Reactors 3, 4, 7, and 8 continued to maintain low levels of dissolved iron throughout phase 2. For reactors with iron chemistry controlled by the sulfide (R3, R4, and R7), Figure 3 illustrates how these reactors continued to lose the sulfate and, therefore, their predominant iron species was predicted to be FeS, produced by the activity of sulfate-reducing microbes [34,59]. Reactor

8 differed in that neither sulfate loss nor dissolved H_2S was detected during Phase 2 until near the end of the experiment (Figure 3). Therefore, the predominant iron species formed during Phase 2 in R8 was predicted to be iron oxides such as magnetite, goethite, and lepidocrocite, together with sulfate green rust ($Fe(II)_4Fe(III)_2(OH)_{12}SO_4 \cdot 8H_2O$) [30].

3.2. Analysis of Coupon Surfaces

3.2.1. EDX

Coupons were removed from the reactors at the conclusion of the experiment (764 days), and their surfaces were examined to identify the elements present in the corrosion products and their relative abundance (Figure S2). Our focus was to determine whether or not some of the corrosion products could be attributed to the activity of sulfate-reducing microorganisms; therefore, we were particularly interested in whether sulfur co-occurred with iron, as that would be consistent with the corrosion product FeS associated with the activity of sulfate-reducing microbes [34,59]. Iron co-occurring with oxygen could be interpreted as indicating iron oxides or a product such as sulfate green rust that contains iron, sulfur, and oxygen [30,31]. The EDX analyses of corrosion products on uncleaned coupons indicated that all coupon surfaces contained oxygen, iron, and sulfur, while carbon was also detected on the coupons from reactors 2, 3, and 4 (Figure S2). On a finer scale, 83/86 individual spectra (each coupon was examined at 8 to 14 different points) contained iron, sulfur, and oxygen, while 3 showed oxygen and iron but no sulfur. Therefore, the EDX results were consistent with corrosion products such as FeS and various iron oxides.

3.2.2. SEM

The coupons were examined using SEM both before and after cleaning, along with the EDX analyses of corrosion products on the uncleaned surfaces. The SEM images of the cleaned coupons show minimal corrosion (no pitting or etching of the surface) of coupons from the reactors that contained only petro F76 fuel or no fuel (R1, R2, R7, R8, Figure 5a). However, pitting was observed on coupons from reactors that contained FT-F76. Coupons from reactors 3 and 4 showed pitting and rough surfaces, and coupons from reactors 5 and 6 had rough surfaces and some pits (Figure 5b).

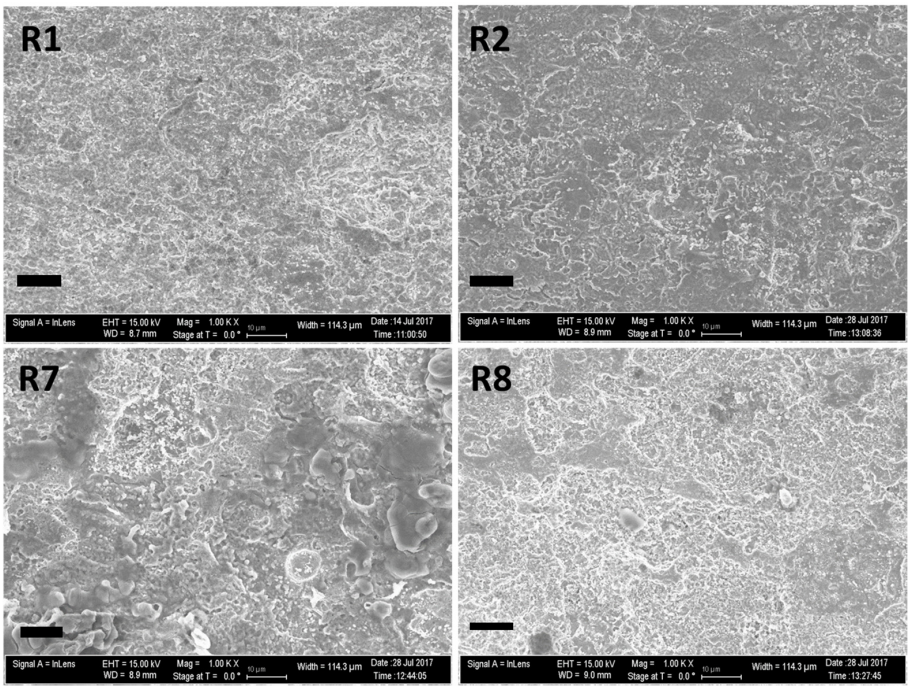

(**a**)

Figure 5. *Cont.*

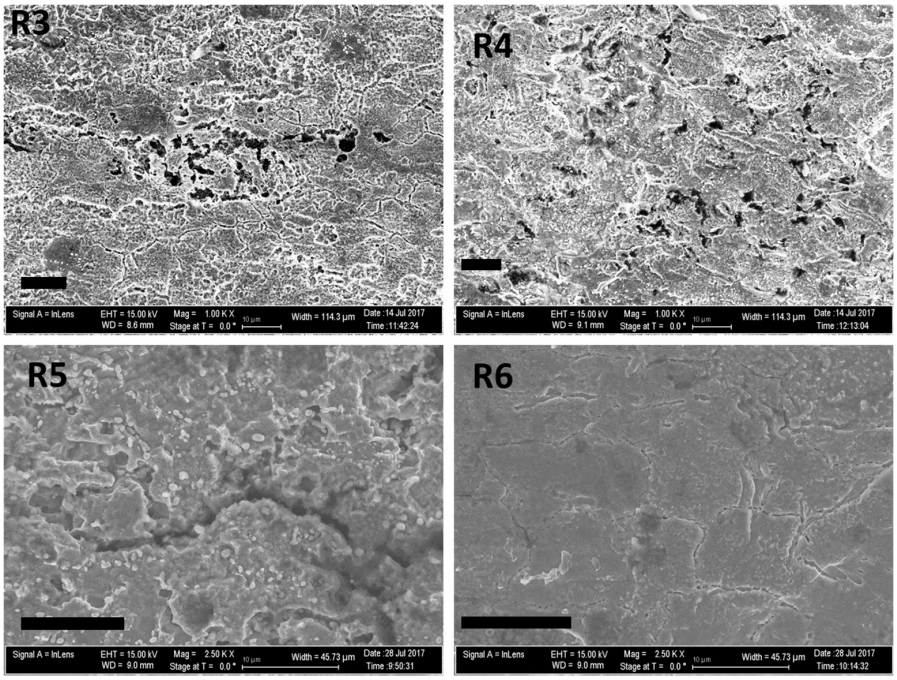

(**b**)

Figure 5. SEM images of cleaned coupons taken from the reactors after 764 days of incubation. Black bar = 10 microns. (**a**) R1 and R2: petro-F76 fuel. R7 and R8: no fuel. (**b**) R3 and R4: FT-F76 fuel. R5 and R6: 1:1 mix of petro-F76 and FT-F76 fuel. See Section 2.3 for more details.

3.3. Microbial Enumeration: qPCR Estimates of # 16S rRNA Gene Copies

The number of bacteria and archaea in the reactors immediately prior to sediment addition was estimated to be in the range of ~10^3 mL^{-1} (R1) 16S rRNA gene copies to ~10^5 mL^{-1}, which is substantially lower than that of the original seawater (1.05×10^6 gene copies mL^{-1}, [18]). The mix of the seawater and sediment added to the reactors at the beginning of phase 2 had an estimated 6.03×10^6 gene copies mL^{-1} and 8.64×10^7 sediment gene copies g^{-1}. The estimated number of bacteria and archaea in water samples at the end of phase 2 ranged from 2.75×10^4 mL^{-1} to 2.23×10^5 mL^{-1} (Figure 6). Note that all reactors that received nonsterile sediments (R1, R3, R5, R7) showed higher # gene copies at the end of phase 2 compared to phase 1 (Table S3). Three of the reactors that received autoclaved sediments had lower numbers at the end of phase 2 compared to phase 1 (R2, R6, R8), and one had higher numbers (R4). The estimated number of bacterial and archaeal 16S rRNA gene copies on the coupons ranged from 2.98×10^5 to 7.87×10^6 g^{-1} of the wet weight of the sample and from 1.58×10^5 to 5.16×10^6 g^{-1} of the wet weight for sediments (Table S4). Estimated copy numbers for the coupons and sediment were higher for the same fuel duplicate that received nonsterile sediment than for the one that received an autoclaved sediment (Table S4).

3.4. Microbial Community Analysis: 16S rRNA Amplicon Libraries

Microbial diversity indices, including species richness ($q = 0$ in the Hill number, 57), exponential Shannon index ($q = 1$), and the inverse Simpson index ($q = 2$, Table S1) of the communities in the reactors sampled at the end of phase 2 showed lower species diversity with a more uneven distribution than that of the seawater/sediment added at the beginning of phase 2. All reactor sediment samples had higher diversity indices than the reactor water or coupon samples, with the highest values from the reactors inoculated with sediment containing living microbiota (R1, R3, R5, R7). Species richness was highest in coupons sampled from reactors inoculated with sediments containing living microbiota and lowest in coupons sampled from the no-fuel reactors (R7, R8).

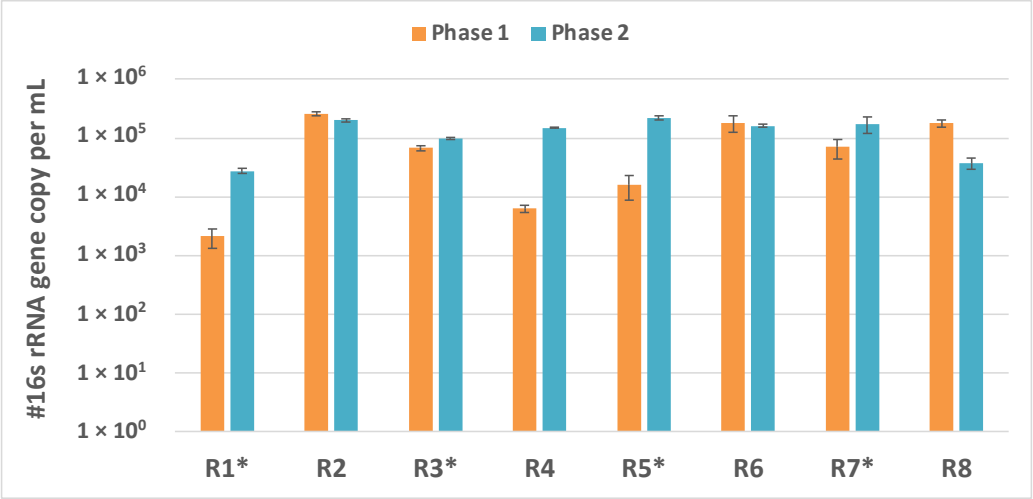

Figure 6. qPCR estimate of the number of 16S rRNA gene copies/mL in water samples collected at the end of phase 1 (orange bars, "Phase 1": immediately before sediment addition) and at the end of phase 2 (blue bars, "Phase 2": approximately 1 year after sediment addition). *: nonsterile sediment added to these reactors; the remaining reactors received autoclaved sediment. R1 and R2: petro-F76 fuel. R3 and R4: FT-F76 fuel. R5 and R6: 1:1 mix of petro-F76 and FT-F76 fuel. R7 and R8: not amended with fuel. Error bars indicate ± 1 standard deviation.

3.4.1. Phase 2 Water Samples

The microbial communities sampled from water and withdrawn from the reactors at the end of phase 2 showed differences among the reactors, particularly in the relative abundance of species known to be sulfate reducers. The sulfate reducers were mainly those identified as members of the classes Desulfobacteria, Desulfovibrionia, and Desulfobulbia within the phylum Desulfobacterota (Figure 7a). The no-fuel reactors (R7, R8) and those containing only FT-F76 fuel (R3, R4) were dominated by Desulfobacterota (R3ph2: 71.4%, R4ph2: 44.5%, R7ph2: 61.3%, R8ph2: 47.4%, Table S4A). Note that the reactors that received nonsterile sediments (R3, R7) had a higher relative abundance of Desulfobacterota than those that received autoclaved sediments (R4, R8). The dominant genera of Desulfobacterota differed between the reactors without fuel and those with FT-F76. Reactors R7 and R8 (no-fuel) contained primarily *Desulfovibrio* (R7: 45.0%, R8: 45.6% relative abundance) while R3 had 43.2% *Desulfonatronum* and R4 had 29.0% *Desulfobacter* (Figure 7a, Table S4B). The relative abundance of *Magnetovibrio*, an iron-sequestering Alphaproteobacteria [60], which at the end of phase 1 dominated in the no-fuel reactors and R4 [18], decreased greatly in the no-fuel reactors but not in R4, when samples were collected after sediment addition (Figure 7a, Table S4B). However, *Magnetovibrio* still made up approximately 25% of the R4 and R8 communities after the addition of the autoclaved sediment.

The reactors that contained petro-F76 (R1, R2) or mixed fuel (R5, R6) had quite different microbial community profiles both before [18] and after the addition of the sediment. After sediment addition, R1 and R5 also diverged from R2 and R6 in OCP, pH, iron, and sulfate levels (Figures 2–4). The reactors that contained petro-F76 (R1, R2) or mixed fuel (R5, R6) differed in terms of whether sediment addition increased the relative abundance of Desulfobacterota (Table S4A). The relative abundance of Desulfobacterota was lower in R1 and R5 after sediment addition, and that of Gammaproteobacteria was higher, but the estimated numbers of both groups were greater due to the higher total number of 16S rRNA gene copies estimated by qPCR (Figure 6). The dominant genera of sulfate/thiosulfate/sulfur-reducing bacteria in R1 changed after sediment addition, with the relative abundance of *Desulfovibrio* being lower, while *Desulfotignum*, *Desulfatitalea*, and *Dethiosulfatibacter* (Firmicutes) became relatively more abundant (Figure 7a, Table S4B). The reverse occurred in R5 after sediment addition; the relative abundance of *Desulfovibrio* increased while that

of *Desulfobacter* and *Desulfotalea* decreased (Table S4B). The major Gammaproteobacteria in R1ph2 were *Immundisolibacter*, *Pseudoalteromonas*, and *Marinobacter*, while *Marinobacter* made up 38.2% in R5ph2.

By contrast, R2 and R6, which were distinguished before sediment addition from the other reactors by their high relative abundance of sulfur-oxidizing Campylobacterota [18], had a much lower relative abundance of these organisms after sediment addition (Table S4A). R2 nearly doubled its relative abundance of Desulfobacterota after sediment addition, with much of this increase due to a greater relative abundance of Desulfosarcinaceae (Table S4B). The relative abundance of Desulfosarcinaceae also increased in R6 but to a lesser extent (Table S4B). While the overall relative abundance of Desulfobacterota in R6 showed little change, *Desulfoluna* and Desulfosarcinaceae increased in their relative abundance while *Synthrophotalea* decreased. R6 had a substantial relative abundance (28.6%) of the Gram-positive *Desulfitibacter* after sediment addition. The relative abundance of Gammaproteobacteria decreased for both R2 and R6 (Table S4A), and there was no increase in the relative abundance of aerobic hydrocarbon-degrading Gammaproteobacterial genera as seen in R1 and R5, although *Marinobacter* was present. However, R2 had a two times higher relative abundance of Alphaproteobacteria (Table S4A), primarily due to an increase in the aerobic hydrocarbon-degrading *Parvibaculum* (Table S4B).

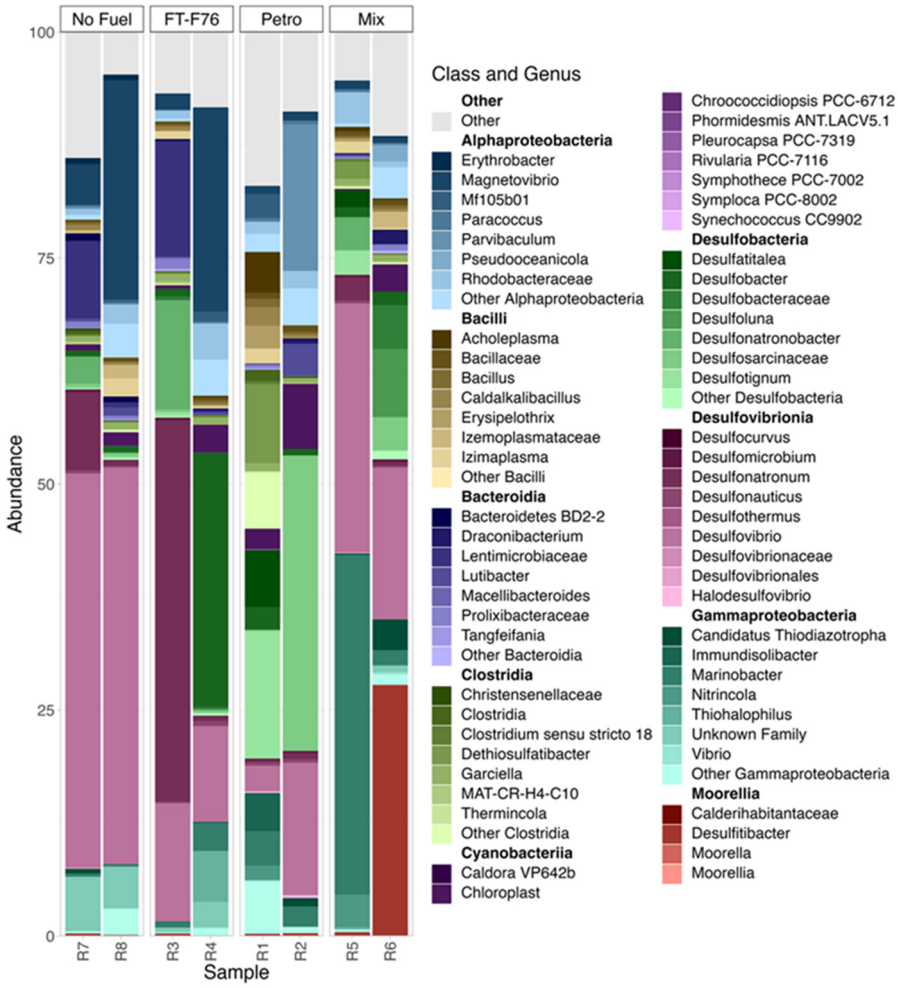

(**a**)

Figure 7. *Cont.*

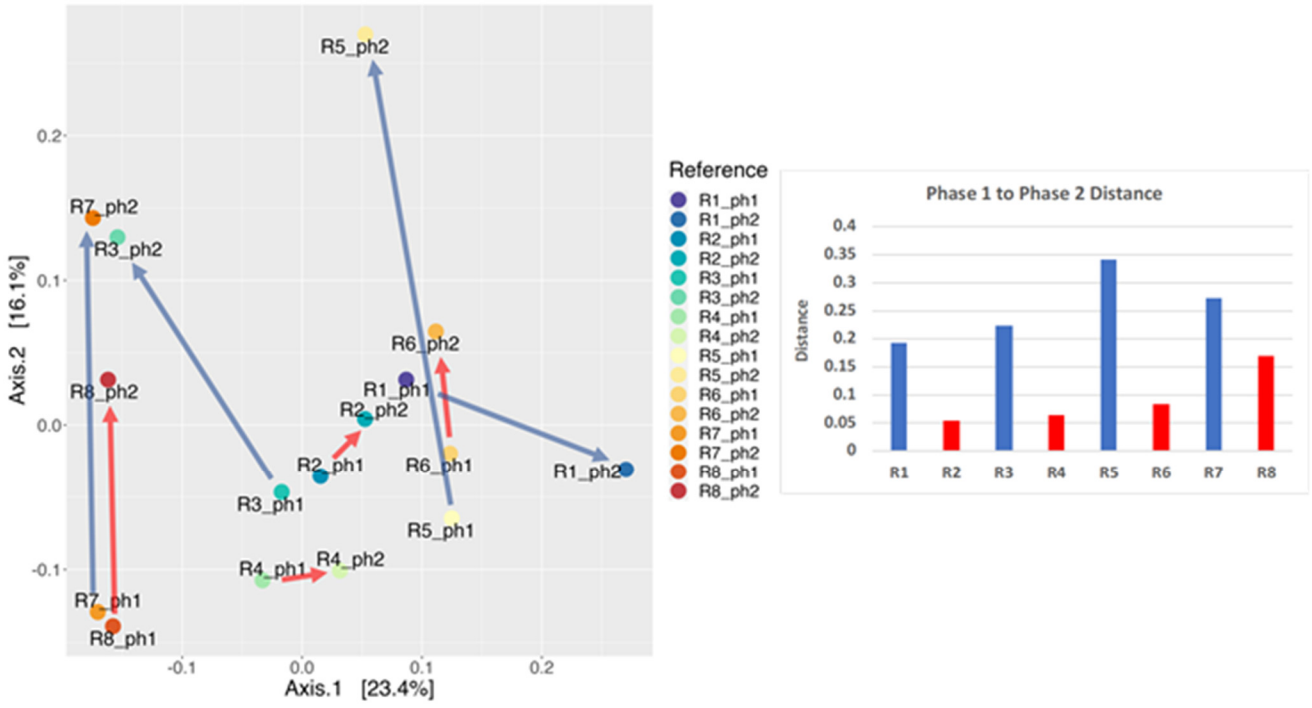

(**b**) (**c**)

Figure 7. (**a**) Bar plot using the top taxa to represent the relative abundance of the top 9 classes and the top 7 genera from the water samples taken at the end of phase 2. The colors signify a top taxonomic rank (class) and the gradient of shades and tints signifies levels at a nested taxonomic rank (genus). (**b**) Principal coordinates analysis (PCoA) of the 16S amplicon libraries from phase 1 and 2 water samples at the genus level using Unifrac weighted distances. (**c**) Bars represent the distance between samples of the same reactor in phase 1 and phase 2. The distance between phase 1 and phase 2 samples was calculated from Axis 1–Axis 2 coordinates, as shown in Figure 7b. Blue bars and arrows represent distances between the samples from reactors that received sediments with live microbiota at the beginning of phase 2; red bars and arrows represent the distances between samples from reactors that received an autoclaved sediment at the beginning of phase 2. R1 and R2: petro-F76 fuel. R3 and R4: FT-F76 fuel. R5 and R6: 1:1 mix of petro-F76 and FT-F76 fuel. R7 and R8: not amended with fuel.

3.4.2. Comparison of Microbial Communities from Phase 1 and Phase 2 Water Samples

Although all phase 1 and their corresponding phase 2 water samples had different community profiles, the samples from reactors that received sediment with live microbiota changed more than the ones that were amended with the autoclaved sediment. Figure 7b shows the location of phase 1 and phase 2 water samples on a principal coordinate analysis (PCoA) plot. The arrows show the change between phase 1 and phase 2 and, therefore, can be quantified as the vector distance between the two samples. Figure 7c shows the plot of the vector distance between phase 1 and phase 2 samples for pairs of reactors that received either nonsterile or autoclaved sediment. Reactors that received sediment with live microbiota (R1, R3, R5, and R7) had a greater distance between their phase 1 and phase 2 water samples than did the reactors that were amended with autoclaved sediment (R2, R4, R6, and R8; *t*-test (paired, 1-tail), $p = 0.008$). Note that although the community composition changed for all reactors from phase 1 to phase 2, R7 and R8 (no-fuel reactors) followed parallel trajectories, in contrast to the continued divergence between the petro-F76 pair (R1, R2) and the FT-F76 pair (R3, R4). The community composition of pairs of reactors containing the same fuel was more dissimilar at the end of phase 2 than it was at the end of phase 1.

3.5. Microbial Communities in Reactor Sediment Samples and on Coupon Surfaces

As noted previously (Section 3.4), the microbial communities of the reactor sediment samples had the highest values of diversity and evenness (Table S1) of the three sample types. The R5sed sample had less than the threshold number of reads and was not analyzed. Desulfobacterota (Figure 8 includes classes Desulfobacteria, Desulfovibrionia, and Desulfobulbia) was the phylum with the highest relative abundance of the sediment samples, ranging from 21.6% (R6sed) to 45.9% (R2sed, Table S5A). Few genera were present with an >5% relative abundance, although *Desulfovibrio* was at >5% in all sediment samples (highest at 18–22% in R2sed, R7sed and R8sed) while chloroplast was >5% in R4sed, R6sed, and R8sed (Figure 8, Table S5A). Note that the relative abundance of Desulfobacterota was considerably lower in the sediment (Table S5A) than in the corresponding water samples (Table S4A) and much lower than in the corresponding coupon samples (Table S5C), with the exception of R1 (R1sed: 29.4%, R1ph2: 30.7%) where the difference was small.

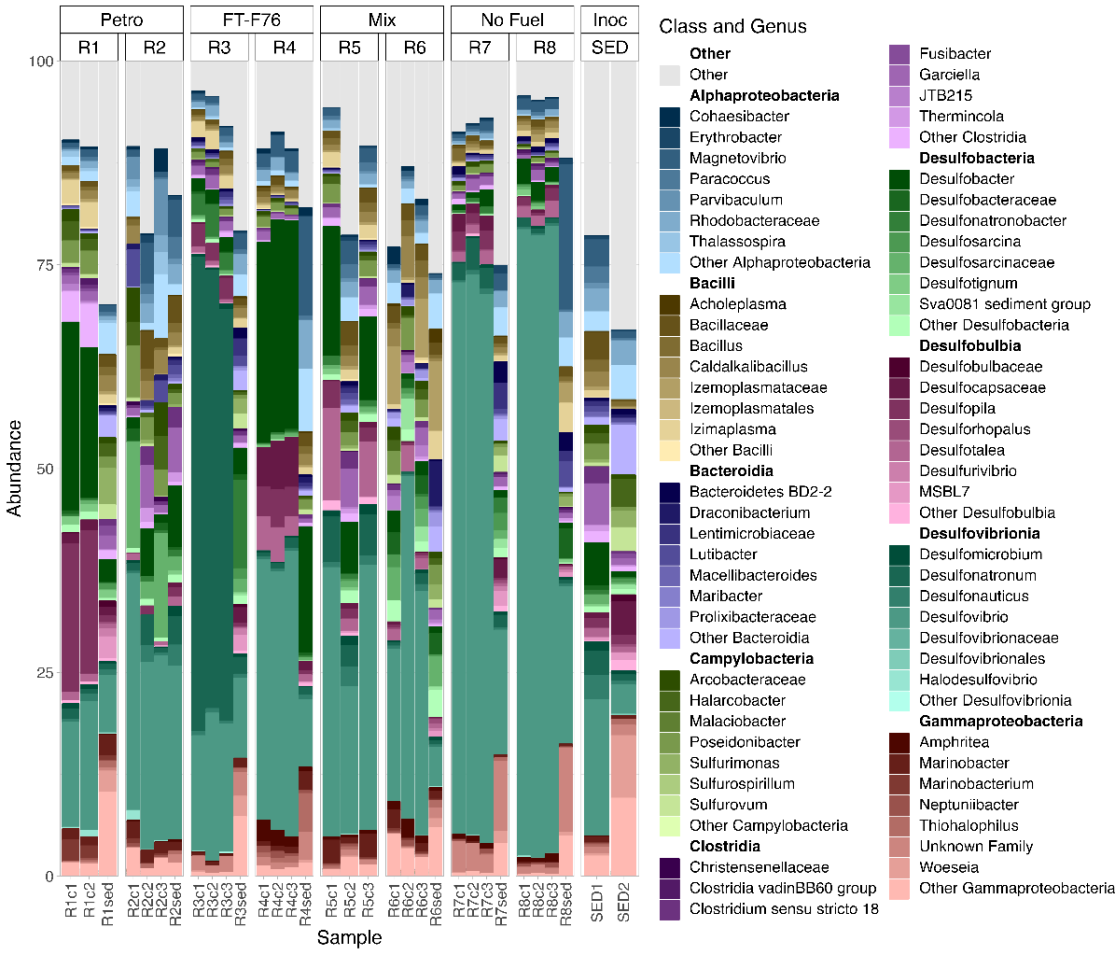

Figure 8. Bar plot using the top taxa to represent the relative abundance of the top 9 classes and the top 7 genera from samples taken at the end of phase 2. The colors signify a top taxonomic rank (class) and the gradient of shades and tints signifies levels at a nested taxonomic rank (genus). SED: marine sediment samples. sed: reactor sediment samples. c: coupon samples. R1 and R2: petro-F76 fuel. R3 and R4: FT-F76 fuel. R5 and R6: 1:1 mix of petro-F76 and FT-F76 fuel. R7 and R8: not amended with fuel.

In contrast to the reactor sediment samples, the coupon surface communities had lower evenness and diversity values (Table S1), with coupons from the no-fuel reactors (R7, R8) and FT-F76 fuel (R3, R4) being the least even/diverse. All coupon samples were dominated by genera in the phylum Desulfobacterota (Figure 8, Table S5C). The replicate

coupons from R3, R4, R7, and R8 were more similar to each other than the coupons from R1, R2, R5, or R6, all of which contained at least 50% petro-fuel (Table S5C,D, Figure 8). *Desulfovibrio* had the highest relative abundance on coupons from the no-fuel reactors R7 (69%) and R8 (77–78%). Coupons from all other reactors contained not only *Desulfovibrio* but also a variety of other Desulfobacterota, such as *Desulfobacter* (especially R1, R4, R5), *Desulfopila* (R1), *Desulfonatronum* (R3), and *Desulfotalea* (R4, R5) (Figure 8, Table S5D).

3.5.1. Coupon Communities Associated with Different Fuel Types

Statistical analysis (one-way ANOVA) of the coupon communities grouped by the type of fuel used (petro-F76: R1, R2; FT-F76: R3, R4; fuel mix: R5, R6; not amended with fuel: R7, R8) revealed 33 taxa with significant differences ($p < 0.05\%$) in relative abundance among the fuel types (Table S6). Most differences were small (3% or less) with the exception of *Desulfovibrio* (74% in no-fuel reactors R7 and R8, <31% in all reactors containing fuel) and *Desulfonatronum* (28% in FT-F76 reactors R3 and R4, <3% in all other reactors). In general, significant (e.g., 0.05 level) taxa were at the lower relative abundance in R3, R4, R7, and R8 and at the higher relative abundance in reactors containing at least some petro-F76 fuel (R1, R2, R5, R6). This was the case for some taxa of Campylobacteria, as previously seen for water phase samples, and for four genera of aerobic hydrocarbon-degrading Gammaproteobacteria (*Halomonas*, *Marinobacteria*, *Marinobacterium*, *Neptunomonas*). The no-fuel reactors (R7, R8) and the FT-F76 reactors (R3, R4) more often had similar relative abundances of the 33 significant taxa than the no-fuel reactors compared to the petro-F76 reactors (R1, R2). The no-fuel reactors and reactors containing only FT-F76 had four taxa with significant differences in relative abundance, while 17 taxa showed significant differences in relative abundance between the no-fuel and petro-F76 reactors. In comparison, the fuel mix reactors (R5, R6) had seven differences in significant taxa with petro-F76-only reactors, none of which included the aerobic hydrocarbon-degrading Gammaproteobacteria; there were 13 differences with the FT-F76 reactors and 2 taxa (*Desulfosarcina* and *Desulfitibacter*) in which the fuel mix had a uniquely significant higher relative abundance.

3.5.2. Coupon Communities Associated with Pitting Corrosion

Although all coupons presumably had iron sulfides present (Section 3.2.1), indicating the importance of both sulfate reduction and generalized corrosion, localized corrosion or pitting was only noted in the presence of FT-F76 fuel (R3, R4, R5, R6) (Section 3.2.2). In contrast to the number of statistically significant differences among the coupon microbial community composition found when grouping the communities according to fuel type (Table S6), only seven taxa showed significant differences (one-way ANOVA, Table S7) associated with coupons from reactors showing at least some pitting corrosion (reactors R3, R4, R5, R6) compared to those without pits (reactors R1, R2, R7, R8). All of the coupons that showed pits were from reactors containing FT-F76. The four taxa that showed a significantly greater relative abundance on the coupons with pits were Actinomarinales (Acidimicrobiia), *Desulfosarcina* (Desulfobacteria), Desulfotalea (*Desulfobulbia*), and Acholeplasma (Bacilli). Most of the seven significant taxa showed only small differences in the % relative abundance between the two groups, with the exception of *Desulfovibrio*, which had a higher mean value in the group that did not show pitting corrosion due simply to its high relative abundance in the no-fuel reactors (R7, R8).

3.6. Comparison of Water, Sediment and Coupon Samples

The genus-level microbial community composition of phase 2 samples from 16S rRNA amplicon libraries is shown as a PCoA plot in Figure 9. Some similarities among different sample types from the same reactor can be noted; however, the patterns are complex. Phase 2 community profiles from fluids are clustered close to the corresponding coupons for the no-fuel reactors (R7 and R8: orange ovals) and for the FT-F76 reactor that received a nonsterile sediment (R3: purple ovals). In contrast, the sediment samples were less similar in the microbial community composition. The observed distribution of sample

types is at least partially due to the trend in the relative abundance of Desulfobacterota (Figures 7 and 8) from the highest in coupons to the lowest in sediment.

For many of the reactors, the microbial community profile in replicate coupon samples was clustered together, with the notable exception of coupons from reactors containing the fuel mix (R5c, R6c, blue arrows). One of the replicate coupons of R6 (mixed fuel) was similar to coupons of R1 (petro-F76 fuel), one coupon of R2 (petro-F76 fuel), and one of the R4 coupons (FT-F76 fuel), suggesting that the mix of fuels was associated with greater variation among their microbial coupon communities. In contrast, microbial communities on coupons from the no-fuel reactors (R7, R8) were clustered closely together (orange oval, Figure 9).

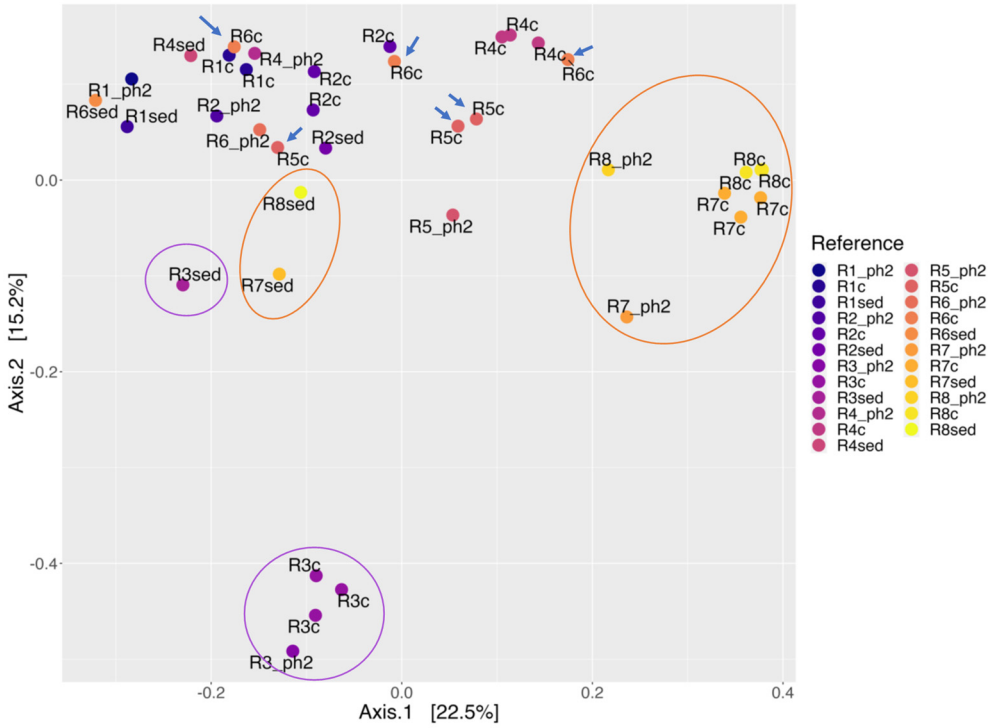

Figure 9. Principal coordinates analysis of the 16S rRNA amplicon libraries from samples taken at the end of phase 2 at the genus level using Bray–Curtis distances. Blue arrows indicate coupons from the mixed fuel reactors, R5 and R6.

4. Discussion

We investigated the effects of adding marine sediments on the development of microbial communities that biodegrade fuel components and enhance steel corrosion in model ballast tank systems.

4.1. Effects of Adding Marine Sediments to Ballast Tanks

A number of changes were observed after the addition of marine sediments to the reactors, including the OCP and pH values (Figure S1 and Figure 2), decreased levels of the dissolved iron and sulfate (Figures 3 and 4), the detection of H_2S (Figure 3), and an increase in the estimated number of 16S rRNA gene copies in water samples taken from R1, R3, R4, R5 and R7 (Figure 6). Changes in the microbial community profiles were greater for reactors receiving nonsterile sediments than those that received autoclaved sediments (Figure 7c), highlighting the contribution made by living sediment microbes.

Microbial community profiles of the water phase samples were strongly impacted by the addition of marine sediment to the seawater-fuel-metal reactors. Most notable were changes in the taxa involved in sulfur cycling and/or hydrocarbon degradation. Before sediment addition, the dominant genus in the no-fuel reactors (water phase) was *Magnetovibrio*,

an iron-sequestering Alphaproteobacteria [60], but after sediment addition, *Desulfovibrio*, a sulfate-reducing bacterium, had the highest relative abundance (approximately 45%, Table S4B). In the reactors containing FT-F76 fuel (R3, R4), the relative abundance of *Desulfovibrio* remained nearly constant (approximately 11 to 13%), but that of other sulfate-reducing bacteria changed. *Desulfobacter* became abundant after sediment addition in R4 but decreased in R3. *Desulfobacter vibrioformis* was isolated from an oil-water separator [61], and all described *Desulfobacter* species can reduce sulfate, with some able to reduce sulfite and thiosulfate [62]. In contrast, *Desulfonatronum* (Desulfonatronaceae) became the dominant taxon in R3 after sediment addition, and *Desulfonatronobacter* (Desulfosarcinaceae) also increased in relative abundance. These organisms are tolerant of alkaline conditions, which is consistent with the pH measured in the reactors after sediment addition (Figure 2b): *Desulfonatronum alkalitolerans* [63] has a pH optimum at 8.5 while *Desulfonatronobacter acidivorans* tolerates pH levels from 8.5 to 10.6 [64]. Both can reduce sulfate and thiosulfate. *Desulfonatronum* can, in addition, reduce sulfite, while some strains of *Desulfonatronum buryatense* can reduce Fe(III) [65].

Reactors amended with petro-F76 (R1, R2) or a mixture of petro-F76 and FT-F76 (R5, R6) showed an increase in the relative proportion of hydrocarbon-degrading taxa. The relative proportion and estimated actual abundance of Gammaproteobacteria in R1 and R5 increased after sediment addition (Table S4B). The more abundant Gammaproteobacteria in R1 (*Immundisolibacter, Pseudoalteromonas, Marinobacter*) are known to be capable of hydrocarbon biodegradation, with *Immundisolibacter cernigliae* [66] and *Pseudoalteromonas* [67] metabolizing polyaromatic hydrocarbons. Various species of *Marinobacter* (at 38% after sediment addition in R5) degrade aliphatic and/or polyaromatic hydrocarbons [68]. *Marinobacter,* in particular, commonly flourishes in oil-contaminated seawater and fuel-compensated ballast tanks [7,67–69].

The reactors R2 and R6, which before sediment addition had a substantial fraction of sulfide oxidizing bacteria [18], after sediment addition showed a marked decrease in these types of organisms, together with an increase in the relative abundance of sulfate/sulfite reducers and taxa noted for hydrocarbon degradation. Desulfosarcinaceae became the most abundant taxon in R2, with *Desulfitibacter* being the most abundant in R6. Desulfosarcinaceae are sulfate-reducing bacteria, while *Desulfitibacter alkalitolerans* is a sulfite reducer [70]. A number of *Desulfosarcina* strains are noted for anaerobic hydrocarbon degradation [16,71–73]. The relative abundance of Gammaproteobacteria decreased for both R2 and R6 (Table S4A), and there was no increase relative to the abundance of aerobic hydrocarbon-degrading Gammaproteobacterial genera as seen in R1 and R5, although *Marinobacter* was present. However, R2 had twice the relative abundance of Alphaproteobacteria (Table S4A), primarily due to an increase in *Parvibaculum* (Table S4B). *P. hydrocarboniclasticum* oxidizes n-alkanes [74], so the water phase of R2 after sediment addition was enriched in microbes with the genetic potential for anaerobic (Desulfosarcinaceae) and aerobic (*Parvibaculum*) hydrocarbon degradation.

4.2. Biodegradation and Biocorrosion Triggered by Addition of Marine Sediments to Fuel-Compensated Ballast Tanks

Our study suggests that the addition of marine sediments to reactors containing seawater, fuel, and carbon steel spurred the biodegradation of fuel components (inferred by an increase in the relative abundance of hydrocarbon-degrading bacteria) and sulfate reduction activity (as indicated by iron sulfides on carbon steel coupons, a decrease in sulfate levels and detection of dissolved H_2S), which, in turn, enhance MIC. However, marine sediments are far more than mere inoculum additions. Sediments contain inorganic and organic materials that promote microbial growth and activity, such as sulfate and sulfur compounds, iron, manganese and other metals, nitrogenous compounds, the remains of organisms, and particulate matter for surface attachment and the formation of biofilms [75–80]. Busy harbors, like the source of the seawater and marine sediments used to inoculate the reactors, also accumulate various xenobiotic materials, including petroleum

products [81]. A variety of microorganisms that degrade petroleum hydrocarbons and other xenobiotic compounds, along with their metabolites, have been isolated from marine sediments, especially from near-shore areas with chronic pollution from marinas [82–86]. Marine sediments and seawater also harbor an array of different physiological types of microbes that could contribute to biocorrosion, including thiosulfate-reducing, sulfate-reducing, iron-oxidizing, iron-reducing, sulfide-oxidizing, and fermenting bacteria as well as methanogens and other microbes [23,25,75–78,86,87].

Many of the taxa at the highest relative abundance in the microbial communities on the carbon steel coupons in this study have been previously associated with the corrosion of metal surfaces (Table S5C,D, Figure 8). These include many sulfate/sulfite/thiosulfate-reducing bacteria belonging to the Desulfobacterota, including sulfur-oxidizing bacteria such as *Halarcobacter* (formerly *Arcobacter*), *Poseidonibacter* and other genera belonging to the family Arcobacteraceae and Fe/S cycling bacteria such as *Syntrophotalea* (formerly *Pelobacter*) or those that may contribute indirectly to MIC through hydrocarbon biodegradation *(Marinobacter, Parvibaculum*, other aerobic hydrocarbon-degrading Gamma- and Alphaproteobacteria, anaerobic hydrocarbon-degraders) and genera belonging to the family Anaerolineaceae.

There were few significant differences in the microbial profiles of samples taken from coupons which showed pitting (R3, R4, R5, R6: all were amended with at least some FT-F76) versus those that did not (R1, R2: amended with petro-F76, R7, R8: not amended with fuel, ANOVA Table S7). The relative abundance of Actinomarinales, *Desulfosarcina*, *Desulfotalea*, and *Acholeplasma* was slightly higher in the reactors that did show pits on their coupons. Sulfate and Fe(III) can be used as electron acceptors by *Desulfotalea* [88], while several strains of *Desulfosarcina* are capable of anaerobic hydrocarbon degradation [16,71–73] as well as being sulfate reducers. However, although a higher relative abundance of these genera was associated with pitting corrosion in this experiment, we must be cautious as this is correlative, not causative evidence, and also as the comparisons included coupons from reactors that differed in fuel type as well as pitting. As detailed above (Section 3.5.1, many more significant differences in the relative abundance of taxa were found for coupon communities grouped by fuel type than whether or not pits were found on the coupons.

As discussed in the Introduction, MIC was promoted by the presence of marine sediments in a laboratory experiment testing a range of naval fuels [21]. Furthermore, the addition of the sediment into reactors containing fuel produced more variation in the microbial community structure than the addition of the sediment to reactors without fuel (Section 3.6). We describe below how the addition of sediments might trigger aerobic hydrocarbon biodegradation and subsequent steel biocorrosion in ballast tanks containing different naval fuels.

4.2.1. Effect of Dissolved Iron on Aerobic Hydrocarbon Degradation

As noted (see Section 4.1), sediments from fuel-polluted harbors contain a variety of hydrocarbon-degrading bacteria, and the process of adding water or sediments to ballast tanks introduces oxygen. We are aware of the roles that various forms of iron may play in promoting anaerobic hydrocarbon degradation [89], but our focus is on aerobic hydrocarbon degradation. That is, we contend that the dissolved iron produced during corrosion processes can stimulate aerobic hydrocarbon degradation in fuel-compensated ballast tanks. The biogeochemical cycling of iron in oceans has been shown to have a profound effect on microbial metabolism. Indeed, iron has been considered a limiting nutrient in many marine systems [90,91]. It is not surprising, therefore, that microbes have a variety of mechanisms to take up both ferrous and ferric iron [92,93]. Various taxa have different genetic potential for iron uptake mechanisms, and at least some commonly encountered aerobic hydrocarbon-degrading bacteria respond rapidly to iron input [43,44]. A particularly important factor in our study is that our reactors did allow a low level of oxygen diffusion (Section 4.1) that was sufficient to support sulfide-oxidizing bacteria and aerobic hydrocarbon-degrading Gamma and Alphaproteobacteria (Section 4.1).

Therefore, a reasonable postulate is that when marine sediments containing the requisite microflora are exposed to both fuel and carbon steel as well as traces of oxygen, corrosion processes result in the production of increased levels of dissolved iron that, in turn, stimulate the aerobic metabolism of susceptible hydrocarbons. With time, conditions become more unfavorable for aerobic heterotrophic respiration since the available oxygen becomes consumed, thereby favoring the development of anaerobic microbial communities that are capable of linking hydrocarbon decay to the reduction in the sulfate and MIC. This potential feedback loop continues until essential nutrients are depleted or waste products accumulate, but such processes may act to enhance MIC by transiently providing the metabolites of aerobic hydrocarbon biodegradation that can subsequently be used by MIC-enhancing anaerobic microbes [45].

We noted a rapid decrease in dissolved iron during phase 2 in R1 and R5, inoculated with live sediments, together with an increase in the relative abundance and estimated absolute abundance of aerobic hydrocarbon-degrading Gammaproteobacteria. There was not as great a drop in dissolved iron (Figure 4) nor as great a rise in the relative abundance of aerobic hydrocarbon-degrading Gammaproteobacteria in the water phase of R2 and R6; these reactors had the same fuel amendments as R1 and R5, respectively, but instead contained a high relative proportion of sulfide-oxidizing taxa, a higher estimated number of bacteria, and were amended with autoclaved sediments. The level of dissolved iron in the reactors containing at least some petro-F76 fuel within the first month after sediment addition (Figure 4, maximum ~ 30,000 ppb in R1, >15,000 in R2, R5, R6) was more than 1000× the iron level determined for the San Diego Harbor seawater used to inoculate the reactors (16.2 ppb, Section 3.1.3) and much greater than the level reported for many offshore surface waters considered to be iron-limited [91,92].

Other studies support our supposition that the level of dissolved iron in some of the reactors was sufficient to enhance aerobic hydrocarbon degradation. Experiments using the supplementation of seawater with iron and other metals, both separately and in combination [43], found that the relative abundance of several genera of aerobic hydrocarbon-degrading bacteria, in particular, *Oleibacter, Martelella, Marinobacter, Alcanivorax, Henriciella, Hyphomonas,* and *Thalassolituus*, increased when the metals were added at 5× the previously observed metal concentration of the seawater (supplemented with iron at 12 nM, or 6.7 ppb). The consumption of the iron and substrate by *Pseudomonas putida* bearing the TOL plasmid (contains genes permitting oxidation of toluene) was compared when grown on toluene under iron-limited (1 μM $FeCl_3$) and iron-excess (10 μM $FeCl_3$) conditions [93]. More iron was consumed, though not 100% of the quantity was added, when cells were grown on toluene with 10 μM of $FeCl_3$ (5584 ppb Fe), suggesting that the iron-excess level was indeed sufficient for microbial growth via the oxidation of this hydrocarbon. Note that the highest iron concentrations seen in R1, R2, R5, and R6 (Figure 4: ~30,000 ppb in R1, >15,000 in R2, R5, and R6) were much higher than the iron-excess level used by Dinkla et al. [93]. The highest dissolved iron concentration, seen 2 days after sediment addition in R3, R4, R7, and R8 (R3: 3832 ppb, Figure 4), was less than the iron-excess but greater than the iron-limitation value, although the iron concentration decreased over time in the reactors (Figure 4). The persistently lower iron levels in R3, R4, R7, and R8 might reflect the continued presence of iron-sequestering *Magnetovibrio* [60] in these reactors (Figure 7a, Table S4B).

4.2.2. Differential Toxicity of Various Fuel Components to Microorganisms

In a previous field study of fuel-compensated ballast tanks with different shipboard residence times, it was noted that aerobic hydrocarbon biodegradation preceded the anaerobic biodegradation of fuel components ([7], see also Introduction). In a study with reactors containing seawater, fuel, and carbon steel coupons, the transient exposure to oxygen allowed the aerobic biodegradation of fuels, which provided intermediates for anaerobic processes, resulting in the sulfide production and corrosion of the carbon steel [45].

However, an early bloom of aerobic hydrocarbon degraders might also ultimately promote anaerobic metabolism by reducing the toxicity of fuel components to anaerobic bacteria. The compounds present in fuels are toxic to microorganisms [94], with the degree of toxicity being both dose-dependent and generally proportional to the chemical's octanol/water partitioning coefficient (K_{OW}), although bioavailability is affected by a number of other factors [95]. The K_{OW} predicts partitioning into cell membranes, which increases the fluidity and, therefore, the permeability of the membrane [94,95]. As noted by Duldhardt et al. [47], in a study on the effect of adding various organic solvents, including some hydrocarbons present in fuels (BTEX: benzene, toluene, ethylbenzene, xylene) to exponentially growing cultures, the growth of three anaerobic bacteria, *Thauera aromatica*, *Desulfococcus multivorans* and *Geobacter sulfurreducens* was inhibited at much lower levels of the test chemicals than the growth of aerobic hydrocarbon-degrading *Pseudomonas putida*. This study [47] found that the sensitivity of *P. putida* was similar to values in the literature for *Escherichia coli* and *Acinetobacter calcoaceticus*; thus, *P. putida* was not unique in being less sensitive than the anaerobic bacteria. Therefore, a second consequence of the aerobic hydrocarbon biodegradation of more toxic fuel components in a marine setting may be to facilitate subsequent anaerobic metabolism, including sulfate reduction and MIC.

4.2.3. Effect of Fuel Composition on Biodegradability and Corrosion

Petro-F76 fuel had a higher proportion of linear alkanes (C8–C12, C13–C24), cycloalkanes, alkylated benzenes, and alkylated naphthalene than FT-F76 while FT-F76 had a high relative abundance of iso-alkanes (branched alkanes, [19,21]). It is, therefore, not surprising that petro-F76 and FT-F76 fuels have been shown to differ in their biodegradability and have the potential to exacerbate the corrosion of carbon steel [21]. When fuels and metals were incubated under sulfate-reducing conditions in seawater and the sediment from San Diego Harbor [21], incubation with petro-F76 produced alkylbenzene succinates in the C13–C16 range, indicating the anaerobic metabolism of alkylbenzenes. Previous studies documented that enrichments established under sulfate-reducing conditions from San Diego Harbor sediments could degrade n-alkanes and polycyclic aromatic compounds [82–84,96–98]. The metabolite and gene diagnostics of a variety of aerobic and anaerobic degradative processes were obtained from samples taken from ballast tanks containing petro-F76 fuel and San Diego Harbor seawater, confirming that conditions in the fuel-compensated ballast tanks were conducive to the biodegradation of many components of petro-F76 fuel [7]. A sample taken from a ballast tank filled one week previously contained dissolved oxygen, a microbial profile enriched with aerobic hydrocarbon-degrading Gammaproteobacteria, and metabolites resulting from aerobic hydrocarbon degradation. Samples taken from ballast tanks that were refilled months previously had no detectable oxygen, a microbial profile enriched with sulfate-reducing bacteria, metabolites resulting from anaerobic hydrocarbon degradation, and EDX-analyzed sulfide particulates of iron, copper, and nickel, indicating corrosion linked to sulfate-reduction [7].

There are not nearly as many studies on the biodegradation of FT-F76 fuels. No alkylbenzene succinates were found in the incubations with FT-F76 under sulfate-reducing conditions, but the sulfate lost was calculated to be 4 to 5 times more than necessary to oxidize all the C6–C12 linear alkanes present in the FT-F76 added, suggesting that other portions of the fuel were subject to degradation [21]. Iso-alkanes, which make up more than 50% of the FT-F76 fuel used in these experiments [18,21], and the current experiments are considered more difficult to biodegrade [22,23]. The metabolism of iso-alkanes has been reported under methanogenic conditions from both high-temperature petroleum reservoirs [99] and oil sands tailings [100], using iso-alkanes up to the chain length of 2-methyloctane, which is well below the chain length of the most abundant class of iso-alkanes (C11–C20) in the FT-F76 fuel used for amending the reactors.

A number of studies, however, have been performed on the biodegradation of isoprenoids. Isoprenoids are branched chain-unsaturated alkanes found in crude oil and derived from a variety of bacteria, algae, and other plants [101,102]. Although consid-

ered to be less readily metabolized than n-alkanes of the same chain length [22], the biodegradation of the isoprenoids phytane (2,6,10,14-tetramethylhexadecane) and pristane (2,6,10,14-tetramethylpentadecane) have been reported under aerobic [103–105], nitrate-reducing [106] and sulfate-reducing conditions [107]. Of particular relevance to the current study are reports of biodegradation by marine Gammaproteobacteria taxa that were found in abundance in fuel-compensated ballast tanks [7] and in our reactors. Pristane was readily degraded under aerobic conditions by *Marinobacter hydrocarbonoclasticus* [68] and by the obligate hydrocarbonoclastic marine bacterium *Alcanivorax borkumensis* [108,109]. Intriguingly, Hara et al. [108] suggested that *Alcanivorax* owed its ubiquity in marine waters to its ability to readily degrade branched alkanes. A second alkane degradation pathway was expressed when the *A. bokumensis* strain SK2T was grown on pristane rather than n-alkanes [109]. Screening for gene sequences and coding for enzymes preferentially expressed during pristane degradation in incubations containing FT-F76 may reveal other degraders of branched alkanes. However, it could be difficult to distinguish between sequences in other taxa that code for branched alkane degradation and sequences coding for n-alkane degradation enzymes. It is also necessary to experimentally confirm that the proposed microorganisms can degrade the iso-alkane components present in FT-F76.

The general and pitting corrosion of the incubated carbon steel coupons were seen for both petro-F76 and FT-F76 incubations under strict sulfate-reducing conditions in a previous study, although the loss of sulfate was much greater for the incubations containing petro-F76 fuel [21]. In contrast, our incubations experienced a low rate of oxygen diffusion, which permitted the growth of aerobic microbes, including some aerobic hydrocarbon degraders, but showed pitting corrosion only on carbon steel coupons from reactors containing at least some FT-F76 fuel. With oxygen present, we argued that both fuels likely undergo some degree of aerobic biodegradation, which could produce intermediates for anaerobic processes, resulting in sulfide production and the corrosion of carbon steel, as described previously [45].

5. Conclusions and Recommendations

The marine sediment added to the model reactors was associated with a host of changes in the reactors, including the loss of dissolved iron and sulfate from the water phase, an increase in dissolved H_2S, an increase in the estimated gene copy number in many of the reactors, and a variety of changes in the microbial community composition, including measures of diversity and evenness. Changes in microbial community composition were greater for reactors that received untreated (nonsterile) sediments than those that were amended with autoclaved sediments. Particularly notable was a general increase in the relative abundance of sulfate-reducing bacteria and of the genera noted for aerobic or anaerobic hydrocarbon degradation in reactors containing fuel.

From a pragmatic standpoint, it is crucial to prevent the introduction of marine sediments into fuel-compensated ballast tanks. This may be accomplished through a variety of means, but to draw compensation water away from near-shore fuel-polluted harbors seems advisable. Additionally, monitoring for blooms of aerobic hydrocarbon-degrading bacteria may provide an early warning of fuel degradation and successional processes leading to MIC, while an increase in dissolved H_2S may be of value as an early indicator of MIC.

Supplementary Materials: The following supporting information can be downloaded at: https://www.mdpi.com/article/10.3390/cmd5010001/s1; Figure S1: OCP and pH values over time; Figure S2: EDX analysis of coupons; Table S1: Alpha diversity measurements for 16S rRNA amplicon libraries; Table S2: Sulfur parameters; Table S3: qPCR estimates of bacterial and archaeal 16S rRNA gene copies; Table S4: Microbial community composition of water samples; Table S5: Microbial community composition of sediment and coupon samples; Table S6: ANOVA of coupon microbial composition by fuel type; Table S7: ANOVA of coupon microbial composition by presence/absence of pitting corrosion.

Author Contributions: Conceptualization, K.E.D., M.A.N., I.A.D. and J.M.S.; Data curation, K.E.D., L.E.D., I.A.D. and B.H.H.; Formal analysis, K.E.D., L.E.D., M.A.N., I.A.D. and B.H.H.; Funding acquisition, J.M.S.; Methodology, K.E.D. and M.A.N.; Project administration, J.M.S.; Supervision, K.E.D., M.A.N., I.A.D. and J.M.S.; Writing—original draft, K.E.D. and L.E.D.; Writing—review and editing, K.E.D., L.E.D., M.A.N., I.A.D., B.H.H. and J.M.S. All authors have read and agreed to the published version of the manuscript.

Funding: This research was funded by the Office of Naval Research, award number N000141010946.

Data Availability Statement: All amplicon library sequences were deposited in the NCBI Sequence Read Archive under Bioproject accession number PRJNA875099.

Acknowledgments: We would like to acknowledge the technical assistance of Athenia Oldham, Charles Primeaux, and Ravi Garimella. Chris Marks collected the seawater used in these experiments. Commander Heidi Boose, USN, facilitated access to these samples.

Conflicts of Interest: The authors declare no conflicts of interest.

References

1. Ruiz, G.M.; Rawlings, T.K.; Dobbs, F.C.; Drake, L.A.; Mullady, T.; Huq, A.; Colwell, R.R. Global spread of microorganisms by ships. *Nature* **2000**, *408*, 49–50. [CrossRef] [PubMed]
2. Drake, L.A.; Doblin, M.A.; Dobbs, F.C. Potential microbial bioinvasions via ships' ballast water, sediment, and biofilm. *Mar. Pollut. Bull.* **2007**, *55*, 333–341. [CrossRef] [PubMed]
3. Burkholder, J.M.; Hallegraeff, G.M.; Melia, G.; Cohen, A.; Bowers, H.A.; Oldach, D.W.; Parrow, M.W.; Sullivan, M.J.; Zimba, P.V.; Allen, E.H.; et al. Phytoplankton and bacterial assemblages in ballast water of U.S. military ships as a function of port of origin, voyage time, and ocean exchange practices. *Harmful Algae* **2007**, *6*, 486–518. [CrossRef]
4. Xue, Z.; Tian, W.; Han, Y.; Feng, Z.; Wang, Y.; Zhang, W. The hidden diversity of microbes in ballast water and sediments revealed by metagenomic sequencing. *Sci. Total Environ.* **2023**, *882*, 163666. [CrossRef] [PubMed]
5. Heyer, A.; D'Souza, F.; Morales, C.F.L.; Ferrari, G.; Mol, J.M.C.; De Wit, J.H.W. Ship ballast tanks a review from microbial corrosion and electrochemical point of view. *Ocean Eng.* **2013**, *70*, 188–200. [CrossRef]
6. Güney, C.B.; Danışman, D.B.; Bozkurtoğlu, S.N.E. Reduction of ballast tank sediment: Evaluating the effect of minor structural changes and developing a pneumatic cleaning system. *Ocean Eng.* **2020**, *203*, 107204. [CrossRef]
7. Marks, C.R.; Duncan, K.E.; Nanny, M.A.; Harriman, B.H.; Avci, R.; Oldham, A.L.; Suflita, J.M. An integrated metagenomic and metabolite profiling study of hydrocarbon biodegradation and corrosion in navy ships. *NPJ Mater. Degrad.* **2021**, *5*, 60. [CrossRef]
8. Maglić, L.; Frančić, V.; Zec, D.; David, M. Ballast water sediment management in ports. *Mar. Pollut. Bull.* **2019**, *147*, 237–244. [CrossRef]
9. Feng, D.; Chen, X.; Tian, W.; Qian, Q.; Shen, H.; Liao, D.; Lv, B. Pollution characteristics and ecological risk of heavy metals in ballast tank sediment. *Environ. Sci. Pollut. Res.* **2017**, *24*, 3951–3958. [CrossRef]
10. Hamer, J.P. Ballast Tank Sediments. In *Invasive Aquatic Species of Europe. Distribution, Impacts and Management*; Leppäkoski, E., Gollasch, S., Olenin, S., Eds.; Kluwer Academic Publishers: Dordrecht, The Netherlands, 2002; pp. 232–234.
11. Lv, B.; Cui, Y.; Tian, W.; Feng, D. Composition and influencing factors of bacterial communities in ballast tank sediments: Implications for ballast water and sediment management. *Mar. Environ. Res.* **2017**, *132*, 14–22. [CrossRef]
12. Lv, B.; Shi, J.; Li, T.; Ren, L.; Tian, W.; Lu, X.; Han, Y.; Cui, Y.; Jiang, T. Deciphering the characterization, ecological function and assembly processes of bacterial communities in ship ballast water and sediments. *Sci. Total Environ.* **2022**, *816*, 152721. [CrossRef] [PubMed]
13. Cleland, J.H. Corrosion risks in ships´ ballast tanks and the IMO pathogen guidelines. *Eng. Failure Anal.* **1995**, *2*, 79–84. [CrossRef]
14. Van Hamme, J.D.; Singh, A.; Ward, O.P. Recent advances in petroleum microbiology. *Microbiol. Mol. Biol. Rev.* **2003**, *67*, 503–549. [CrossRef] [PubMed]
15. Kostka, J.E.; Teske, A.P.; Joye, S.B.; Head, I.M. The metabolic pathways and environmental controls of hydrocarbon biodegradation in marine ecosystems. *Front. Microbiol.* **2014**, *5*, 471. [CrossRef] [PubMed]
16. Davidova, I.A.; Marks, C.R.; Suflita, J.M. Anaerobic Hydrocarbon-Degrading Deltaproteobacteria. In *Taxonomy, Genomics and Ecophysiology of Hydrocarbon-Degrading Microbes. Handbook of Hydrocarbon and Lipid Microbiology*; McGenity, T., Ed.; Springer: Cham, Switzerland, 2018. [CrossRef]
17. Rabus, R.; Boll, M.; Heider, J.; Meckenstock, R.U.; Buckel, W.; Einsle, O.; Ermler, U.; Golding, B.T.; Gunsalus, R.P.; Kroneck, P.M.; et al. Anaerobic Microbial Degradation of Hydrocarbons: From Enzymatic Reactions to the Environment. *J. Mol. Microbiol. Biotechnol.* **2016**, *26*, 5–28. [CrossRef] [PubMed]
18. Dominici, L.E.; Duncan, K.E.; Nanny, M.A.; Davidova, I.A.; Harriman, B.H.; Suflita, J.M. Microbial Communities Associated with Alternative Fuels in Model Seawater-Compensated Fuel Ballast Tanks. *Corros. Mater. Degrad.* **2023**, *4*, 382–397. [CrossRef]
19. Stamper, D.M.; Lee, G.L. *The Explicit and Implicit Qualities of Alternative Fuels: Issues to Consider for Their Use in Marine Diesel Engines*; Technical Report NSWCCD-61-TR–2008/15; Naval Surface Warfare Center: West Bethesda, MD, USA, 2008.

20. Leckel, D. Diesel production from Fischer-Tropsch: The past, the present, and new concepts. *Energy Fuels* **2009**, *23*, 2342–2358. [CrossRef]
21. Liang, R.; Aktas, D.F.; Aydin, E.; Bonifay, V.; Sunner, J.; Suflita, J.M. Anaerobic Biodegradation of Alternative Fuels and Associated Biocorrosion of Carbon Steel in Marine Environments. *Environ. Sci. Technol.* **2016**, *50*, 4844–4853. [CrossRef]
22. Atlas, R.M. Microbial degradation of petroleum hydrocarbons: An environmental perspective. *Microbiol. Rev.* **1981**, *45*, 180–209. [CrossRef]
23. Xue, J.; Yu, Y.; Bai, Y.; Wang, L.; Wu, Y. Marine Oil-Degrading Microorganisms and Biodegradation Process of Petroleum Hydrocarbon in Marine Environments: A Review. *Curr. Microbiol.* **2015**, *71*, 220–228. [CrossRef]
24. Liang, R.; Grizzle, R.S.; Duncan, K.E.; McInerney, M.J.; Suflita, J.M. Roles of thermophilic thiosulfate-reducing bacteria and methanogenic archaea in the biocorrosion of oil pipelines. *Front. Microbiol.* **2014**, *5*, 89. [CrossRef] [PubMed]
25. Vigneron, A.; Alsop, E.B.; Chambers, B.; Lomans, B.P.; Head, I.M.; Tsesmetzis, N. Complementary Microorganisms in Highly Corrosive Biofilms from an Offshore Oil Production Facility. *Appl. Environ. Microbiol.* **2016**, *82*, 2545–2554. [CrossRef] [PubMed]
26. Lee, J.S.; Little, B.J. Diagnosing microbiologically influenced corrosion. In *Microbiologically Influenced Corrosion in the Upstream Oil and Gas Industry*, 1st ed.; Enning, D., Jason, L., Skovhus, T.L., Eds.; CRC Press: Boca Raton, FL, USA, 2017.
27. Little, B.J.; Hinks, J.; Blackwood, D.J. Microbially influenced corrosion: Towards an interdisciplinary perspective on mechanisms. *Int. Biodeterior. Biodegrad.* **2020**, *154*, 105062. [CrossRef]
28. Knisz, J.; Eckert, R.; Gieg, L.M.; Koerdt, A.; Lee, J.S.; Silva, E.R.; Skovhus, T.L.; An Stepec, B.A.; Wade, S.A. Microbiologically influenced corrosion-more than just microorganisms. *FEMS Microbiol. Rev.* **2023**, *47*, fuad041. [CrossRef] [PubMed]
29. Ulrich, G.A.; Krumholz, L.R.; Suflita, J.M. A rapid and simple method for estimating sulfate reduction activity and quantifying inorganic sulfides. *Appl. Environ. Microbiol.* **1997**, *63*, 1627–1630. [CrossRef] [PubMed]
30. Refait, P.; Grolleau, A.-M.; Jeannin, M.; Rémazeilles, C.; Sabot, R. Corrosion of carbon steel in marine environments: Role of the corrosion product layer. *Corros. Mater. Degrad.* **2020**, *1*, 198–218. [CrossRef]
31. Rémazeilles, C.; Lévêque, F.; Conforto, E.; Refait, P. Long-term alteration processes of iron fasteners extracted from archaeological shipwrecks aged in biologically active waterlogged media. *Corros. Sci.* **2021**, *181*, 109231. [CrossRef]
32. Braunschweig, J.; Bosch, J.; Meckenstock, R.U. Iron oxide nanoparticles in geomicrobiology: From biogeochemistry to bioremediation. *New Biotechnol.* **2013**, *30*, 793–802. [CrossRef]
33. Xia, D.-H.; Deng, C.-M.; Macdonald, D.; Jamali, S.; Mills, D.; Luo, J.-L.; Strebl, M.G.; Amiri, M.; Jin, W.; Song, S.; et al. Electrochemical measurements used for assessment of corrosion and protection of metallic materials in the field: A critical review. *J. Mater. Sci. Technol.* **2022**, *112*, 151–183. [CrossRef]
34. Ferris, F.G.; Jack, T.R.; Bramhill, B.J. Corrosion products associated with attached bacteria at an oil field water injection plant. *Can. J. Microbiol.* **1992**, *38*, 1320–1324. [CrossRef]
35. Lovley, D.R. Dissimilatory Fe(III) and Mn(IV) reduction. *Microbiol. Rev.* **1991**, *55*, 259–287. [CrossRef] [PubMed]
36. Fortin, D.; Langley, S. Formation and occurrence of biogenic iron-rich minerals. *Earth-Sci. Rev.* **2005**, *72*, 1–19. [CrossRef]
37. Fan, D.; Lan, Y.; Paul, G.; Tratnyek, P.G.; Johnson, R.L.; Filip, J.; O'Carroll, D.M.; Garcia, A.N.; Agrawal, A. Sulfidation of iron-based materials: A review of processes and implications for water treatment and remediation. *Environ. Sci. Technol.* **2017**, *51*, 13070–13085. [CrossRef] [PubMed]
38. Etique, M.; Jorand, F.P.; Ruby, C. Magnetite as a precursor for green rust through the hydrogenotrophic activity of the iron-reducing bacteria *Shewanella putrefaciens*. *Geobiology* **2016**, *14*, 237–254. [CrossRef]
39. Pineau, S.; Sabot, R.; Quillet, L.; Jeannin, M.; Caplat, C.H.; Dupont-Morral, I.; Refait, P.H. Formation of the Fe(II-III) hydroxysulphate green rust during marine corrosion of steel associated to molecular detection of dissimilatory sulphite-reductase. *Corros. Sci.* **2008**, *50*, 1099–1111. [CrossRef]
40. Lu, Z.; Imlay, J.A. When anaerobes encounter oxygen: Mechanisms of oxygen toxicity, tolerance and defence. *Nat. Rev. Microbiol.* **2021**, *19*, 774–785. [CrossRef] [PubMed]
41. Muyzer, G.; Kuenen, G.; Robertson, L.A. Colorless Sulfur Bacteria. In *The Prokaryotes: Prokaryotic Physiology and Biochemistry*, 4th ed.; Rosenberg, E., DeLong, E.F., Lory, S., Stackebrandt, E., Thompson, F., Eds.; Springer: Berlin/Heidelberg, Germany, 2013; pp. 555–588. [CrossRef]
42. Deng, S.; Wang, B.; Su, S.; Sun, S.; She, Y.; Zhang, F. Dynamics of Microbial Community and Removal of Hydrogen Sulfide (H2S) Using a Bio-Inhibitor and Its Application under the Oil Reservoir Condition. *Energy Fuels* **2022**, *36*, 14128–14135. [CrossRef]
43. Baltar, F.; Gutiérrez-Rodríguez, A.; Meyer, M.; Skudelny, I.; Sander, S.; Thomson, B.; Nodder, S.; Middag, R.; Morales, S.E. Specific Effect of Trace Metals on Marine Heterotrophic Microbial Activity and Diversity: Key Role of Iron and Zinc and Hydrocarbon-Degrading Bacteria. *Front. Microbiol.* **2018**, *9*, 3190. [CrossRef]
44. Denaro, R.; Crisafi, F.; Russo, D.; Genovese, M.; Messina, E.; Genovese, L.; Carbone, M.; Ciavatta, M.L.; Ferrer, M.; Golyshin, P.; et al. *Alcanivorax borkumensis* produces an extracellular siderophore in iron-limitation condition maintaining the hydrocarbon-degradation efficiency. *Mar. Genomics* **2014**, *17*, 43–52. [CrossRef]
45. Aktas, D.F.; Lee, J.S.; Little, B.J.; Duncan, K.E.; Perez-Ibarra, B.M.; Suflita, J.M. Effects of oxygen on biodegradation of fuels in a corroding environment. *Int. Biodeterior. Biodegrad.* **2012**, *81*, 114–126. [CrossRef]
46. Zhang, Y.; Zhai, X.; Guan, F.; Dong, X.; Sun, J.; Zhang, R.; Duan, J.; Zhang, B.; Hou, B. Microbiologically influenced corrosion of steel in coastal surface seawater contaminated by crude oil. *npj Mater. Degrad.* **2022**, *6*, 35. [CrossRef]

47. Duldhardt, I.; Nijenhuis, I.; Schauer, F.; Heipieper, H.J. Anaerobically grown *Thauera aromatica, Desulfococcus multivorans, Geobacter sulfurreducens* are more sensitive towards organic solvents than aerobic bacteria. *Appl. Microbiol. Biotechnol.* **2007**, *3*, 705–711. [CrossRef] [PubMed]
48. Duldhardt, I.; Gaebel, J.; Chrzanowski, L.; Nijenhuis, I.; Härtig, C.; Schauer, F.; Heipieper, H.J. Adaptation of anaerobically grown *Thauera aromatica, Geobacter sulfurreducens* and *Desulfococcus multivorans* to organic solvents on the level of membrane fatty acid composition. *Microb. Biotechnol.* **2010**, *3*, 201–209. [CrossRef] [PubMed]
49. Stern, S.A.; Fried, J.R. Permeability of Polymers to Gases and Vapors. In *Physical Properties of Polymers Handbook*, 2nd ed.; Marks, J.E., Ed.; Springer Science: New York, NY, USA, 2007; pp. 1033–1050.
50. Liang, R.; Suflita, J.M. Protocol for Evaluating the Biological Stability of Fuel Formulations and Their Relationship to Carbon Steel Biocorrosion. In *Hydrocarbon and Lipid Microbiology Protocols*; McGenity, T., Timmis, K., Nogales, B., Eds.; Springer: Berlin/Heidelberg, Germany, 2015; pp. 211–226. [CrossRef]
51. Nordstrom, D.K.; Wilde, F.D. Reduction-oxidation potential (electrode method). In *Techniques of Water-Resources Investigations*; U.S. Geological Survey: Reston, VA, USA, 2005. [CrossRef]
52. Klindworth, A.; Pruesse, E.; Schweer, T.; Peplies, J.; Quast, C.; Horn, M.; Glöckner, F.O. Evaluation of general 16S ribosomal RNA gene PCR primers for classical and next-generation sequencing-based diversity studies. *Nucleic Acids Res.* **2013**, *41*, e1. [CrossRef] [PubMed]
53. Oldham, A.L.; Sandifer, V.; Duncan, K.E. Effects of sample preservation on marine microbial diversity analysis. *J. Microbiol. Methods* **2019**, *158*, 6–13. [CrossRef] [PubMed]
54. Hamady, M.; Walker, J.; Harris, J.; Gold, N.J.; Knight, R. Error-correcting barcoded primers for pyrosequencing hundreds of samples in multiplex. *Nat. Methods* **2008**, *5*, 235–237. [CrossRef] [PubMed]
55. Callahan, B.J.; McMurdie, P.J.; Rosen, M.J.; Han, A.W.; Johnson, A.J.A.; Holmes, S.P. DADA2: High-resolution sample inference from Illumina amplicon data. *Nat. Methods* **2016**, *13*, 581–583. [CrossRef]
56. R Core Team. *R: A Language and Environment for Statistical Computing*; Version 4.2.1; R Foundation for Statistical Computing: Vienna, Austria, 2022; Available online: https://www.R-project.org/ (accessed on 23 June 2022).
57. Hill, M.O. Diversity and Evenness: A Unifying Notation and Its Consequences. *Ecology* **1973**, *54*, 427–432. [CrossRef]
58. McMurdie, P.J.; Holmes, S. Phyloseq: An R package for reproducible interactive analysis and graphics of microbiome census data. *PLoS ONE* **2013**, *8*, e61217. [CrossRef]
59. Enning, D.; Garrelfs, J. Corrosion of iron by sulfate-reducing bacteria: New views of an old problem. *Appl. Environ. Microbiol.* **2014**, *80*, 1226–1236. [CrossRef]
60. Bazylinski, D.A.; Williams, T.J.; Lefèvre, C.T.; Trubitsyn, D.; Fang, J.; Beveridge, T.J.; Moskowitz, B.M.; Ward, B.; Schübbe, S.; Dubbels, B.L.; et al. *Magnetovibrio blakemorei* gen. nov., sp. nov., a magnetotactic bacterium (Alphaproteobacteria: Rhodospirillaceae) isolated from a salt marsh. *Int. J. Syst. Evol. Microbiol.* **2013**, *63*, 1824–1833. [CrossRef] [PubMed]
61. Lien, T.; Beeder, J. *Desulfobacter vibrioformis* sp. nov., a sulfate reducer from a water-oil separation system. *Int. J. Syst. Bacteriol.* **1997**, *47*, 1124–1128. [CrossRef] [PubMed]
62. Tarpgaard, I.H.; Boetius, A.; Finster, K. *Desulfobacter psychrotolerans* sp. nov., a new psychrotolerant sulfate-reducing bacterium and descriptions of its physiological response to temperature changes. *Antonie Van Leeuwenhoek* **2006**, *89*, 109–124. [CrossRef] [PubMed]
63. Sorokin, D.Y.; Tourova, T.P.; Muyzer, G. Isolation and characterization of two novel alkalitolerant sulfidogens from a Thiopaq bioreactor, *Desulfonatronum alkalitolerans* sp. nov., and *Sulfurospirillum alkalitolerans* sp. nov. *Extremophiles* **2013**, *17*, 535–543. [CrossRef] [PubMed]
64. Sorokin, D.Y.; Tourova, T.P.; Panteleeva, A.N.; Muyzer, G. *Desulfonatronobacter acidivorans* gen. nov., sp. nov. and *Desulfobulbus alkaliphilus* sp. nov., haloalkaliphilic heterotrophic sulfate-reducing bacteria from soda lakes. *Int. J. Syst. Evol. Microbiol.* **2012**, *62*, 2107–2113. [CrossRef] [PubMed]
65. Ryzhmanova, Y.; Nepomnyashchaya, Y.; Abashina, T.; Ariskina, E.; Troshina, O.; Vainshtein, M.; Shcherbakova, V. New sulfate-reducing bacteria isolated from Buryatian alkaline brackish lakes: Description of *Desulfonatronum buryatense* sp. nov. *Extremophiles* **2013**, *17*, 851–859. [CrossRef] [PubMed]
66. Corteselli, E.M.; Aitken, M.D.; Singleton, D.R. Description of *Immundisolibacter cernigliae* gen. nov., sp. nov., a high-molecular-weight polycyclic aromatic hydrocarbon-degrading bacterium within the class Gammaproteobacteria, and proposal of Immundisolibacterales ord. nov. and Immundisolibacteraceae fam. nov. *Int. J. Syst. Evol. Microbiol.* **2017**, *67*, 925–931. [CrossRef]
67. Dubinsky, E.A.; Conrad, M.E.; Chakraborty, R.; Bill, M.; Borglin, S.E.; Hollibaugh, J.T.; Mason, O.U.; Piceno, M.Y.; Reid, F.C.; Stringfellow, W.T.; et al. Succession of hydrocarbon-degrading bacteria in the aftermath of the deepwater horizon oil spill in the gulf of Mexico. *Environ. Sci. Technol.* **2013**, *47*, 10860–10867. [CrossRef]
68. Handley, K.M.; Lloyd, J.R. Biogeochemical implications of the ubiquitous colonization of marine habitats and redox gradients by *Marinobacter* species. *Front. Microbiol.* **2013**, *4*, 136. [CrossRef]
69. King, G.M.; Kostka, J.E.; Hazen, T.C.; Sobecky, P.A. Microbial responses to the Deepwater Horizon oil spill: From coastal wetlands to the deep sea. *Ann. Rev. Mar. Sci.* **2015**, *7*, 377–401. [CrossRef]
70. Nielsen, M.B.; Kjeldsen, K.U.; Ingvorsen, K. *Desulfitibacter alkalitolerans* gen. nov., sp. nov., an anaerobic, alkalitolerant, sulfite-reducing bacterium isolated from a district heating plant. *Int. J. Syst. Evol. Microbiol.* **2006**, *56*, 2831–2836. [CrossRef] [PubMed]

71. Chen, S.C.; Ji, J.; Popp, D.; Jaekel, U.; Richnow, H.H.; Sievert, S.M.; Musat, F. Genome and proteome analyses show the gaseous alkane degrader *Desulfosarcina* sp. strain BuS5 as an extreme metabolic specialist. *Environ. Microbiol.* **2022**, *24*, 1964–1976. [CrossRef] [PubMed]
72. Kleindienst, S.; Herbst, F.A.; Stagars, M.; von Netzer, F.; von Bergen, M.; Seifert, J.; Peplies, J.; Amann, R.; Musat, F.; Lueders, T.; et al. Diverse sulfate-reducing bacteria of the Desulfosarcina/Desulfococcus clade are the key alkane degraders at marine seeps. *ISME J.* **2014**, *8*, 2029–2044. [CrossRef] [PubMed]
73. Watanabe, M.; Higashioka, Y.; Kojima, H.; Fukui, M. *Desulfosarcina widdelii* sp. nov. and *Desulfosarcina alkanivorans* sp. nov., hydrocarbon-degrading sulfate-reducing bacteria isolated from marine sediment and emended description of the genus *Desulfosarcina*. *Int. J. Syst. Evol. Microbiol.* **2017**, *67*, 2994–2997. [CrossRef] [PubMed]
74. Rosario-Passapera, R.; Keddis, R.; Wong, R.; Lutz, R.A.; Starovoytov, V.; Vetriani, C. *Parvibaculum hydrocarboniclasticum* sp. nov., a mesophilic, alkane-oxidizing alphaproteobacterium isolated from a deep-sea hydrothermal vent on the East Pacific Rise. *Int. J. Syst. Evol. Microbiol.* **2012**, *62*, 2921–2926. [CrossRef] [PubMed]
75. Burdige, D.J. The biogeochemistry of manganese and iron reduction in marine sediments. *Earth-Sci. Rev.* **1993**, *35*, 249–284. [CrossRef]
76. Jørgensen, B.B.; Findlay, A.J.; Pellerin, A. The Biogeochemical Sulfur Cycle of Marine Sediments. *Front. Microbiol.* **2019**, *10*, 849. [CrossRef]
77. Schmidt, J.M.; Royalty, T.M.; Lloyd, K.G.; Steen, A.D. Potential Activities and Long Lifetimes of Organic Carbon-Degrading Extracellular Enzymes in Deep Subsurface Sediments of the Baltic Sea. *Front. Microbiol.* **2021**, *12*, 702015. [CrossRef]
78. Cravo-Laureau, C.; Duran, R. Marine coastal sediments microbial hydrocarbon degradation processes: Contribution of experimental ecology in the omics'era. *Front. Microbiol.* **2014**, *5*, 39. [CrossRef]
79. Otte, J.M.; Blackwell, N.; Soos, V.; Rughöft, S.; Maisch, M.; Kappler, A.; Kleindienst, S.; Schmidt, C. Sterilization impacts on marine sediment—Are we able to inactivate microorganisms in environmental samples? *FEMS Microbiol. Ecol.* **2018**, *94*, fiy189. [CrossRef]
80. Zhang, C.; Meckenstock, R.U.; Weng, S.; Wei, G.; Hubert, C.R.J.; Wang, J.H.; Dong, X. Marine sediments harbor diverse archaea and bacteria with the potential for anaerobic hydrocarbon degradation via fumarate addition. *FEMS Microbiol. Ecol.* **2021**, *97*, fiab045. [CrossRef] [PubMed]
81. Stransky, C.; Swiderski, M.; Stolzenbach, K.; Isham, B.; Schottle, R.; Rudolph, J.; Tait, K.; Holman, K.; Burruss, A.; Kolb, R.; et al. San Diego Regional Harbor Monitoring Program Final Report. Wood Project No.: 1715100804; San Diego, CA, USA, 2018. Available online: https://pantheonstorage.blob.core.windows.net/environment/Regional-Harbor-Monitoring-Program-2018-Final-Report.pdf (accessed on 23 June 2022).
82. Coates, J.D.; Lonergan, D.J.; Philips, E.J.; Jenter, H.; Lovley, D.R. *Desulfuromonas palmitatis* sp. nov., a marine dissimilatory Fe(III) reducer that can oxidize long-chain fatty acids. *Arch. Microbiol.* **1995**, *164*, 406–413. [CrossRef] [PubMed]
83. Davidova, I.A.; Duncan, K.E.; Choi, O.K.; Suflita, J.M. *Desulfoglaeba alkanexedens* gen. nov., sp. nov., an n-alkane-degrading, sulfate-reducing bacterium. *Int. J. Syst. Evol. Microbiol.* **2006**, *56*, 2737–2742. [CrossRef] [PubMed]
84. Davidova, I.A.; Gieg, L.M.; Duncan, K.E.; Suflita, J.M. Anaerobic phenanthrene mineralization by a carboxylating sulfate-reducing bacterial enrichment. *ISME J.* **2007**, *1*, 436–442. [CrossRef] [PubMed]
85. Davidova, I.A.; Duncan, K.E.; Wiley, G.; Najar, F.Z. *Desulfoferrobacter suflitae* gen. nov., sp. nov., a novel sulphate-reducing bacterium in the Deltaproteobacteria capable of autotrophic growth with hydrogen or elemental iron. *Int. J. Syst. Evol. Microbiol.* **2022**, *72*, 005483. [CrossRef] [PubMed]
86. Yakimov, M.M.; Timmis, K.N.; Golyshin, P.N. Obligate oil-degrading marine bacteria. *Curr. Opin. Biotechnol.* **2007**, *18*, 257–266. [CrossRef]
87. Skovhus, T.L.; Lee, J.S.; Little, B.J. Predominant MIC mechanisms in the oil and gas industry. In *Microbiologically Influenced Corrosion in the Upstream Oil and Gas Industry*; Skovhus, T.L., Enning, E., Lee, J.S., Eds.; CRC Press: Boca Raton, FL, USA, 2017; pp. 75–86. [CrossRef]
88. Knoblauch, C.; Sahm, K.; Jørgensen, B.B. Psychrophilic sulfate-reducing bacteria isolated from permanently cold arctic marine sediments: Description of *Desulfofrigus oceanense* gen. nov., sp. nov., *Desulfofrigus fragile* sp. nov., *Desulfofaba gelida* gen. nov., sp. nov., *Desulfotalea psychrophila* gen. nov., sp. nov. and *Desulfotalea arctica* sp. nov. *Int. J. Syst. Bacteriol.* **1999**, *49*, 1631–1643. [CrossRef]
89. Castro, A.R.; Martins, G.; Salvador, A.F.; Cavaleiro, A.J. Iron Compounds in Anaerobic Degradation of Petroleum Hydrocarbons: A Review. *Microorganisms* **2022**, *10*, 2142. [CrossRef]
90. Tagliabue, A.; Bowie, A.R.; Boyd, P.W.; Buck, K.N.; Johnson, K.S.; Saito, M.A. The integral role of iron in ocean biogeochemistry. *Nature* **2017**, *543*, 51–59. [CrossRef]
91. Tortell, P.D.; Maldonado, M.T.; Granger, J.; Price, N.M. Marine bacteria and biogeochemical cycling of iron in the oceans. *FEMS Microbiol. Ecol.* **1999**, *29*, 1–11. [CrossRef]
92. Debeljak, P.; Toulza, E.; Beier, S.; Blain, S.; Obernosterer, I. Microbial iron metabolism as revealed by gene expression profiles in contrasted Southern Ocean regimes. *Environ. Microbiol.* **2019**, *21*, 2360–2374. [CrossRef] [PubMed]
93. Dinkla, I.J.; Gabor, E.M.; Janssen, D.B. Effects of iron limitation on the degradation of toluene by *Pseudomonas* strains carrying the tol (pWWO) plasmid. *Appl. Environ. Microbiol.* **2001**, *67*, 3406–3412. [CrossRef] [PubMed]

94. Heipieper, H.J.; Neumann, G.; Cornelissen, S.; Meinhardt, F. Solvent-tolerant bacteria for biotransformations in two-phase fermentation systems. *Appl. Microbiol. Biotechnol.* **2007**, *74*, 961–973. [CrossRef] [PubMed]
95. Sikkema, J.; de Bont, J.A.; Poolman, B. Mechanisms of membrane toxicity of hydrocarbons. *Microbiol. Rev.* **1995**, *59*, 201–222. [CrossRef] [PubMed]
96. Coates, J.D.; Anderson, R.T.; Lovley, D.R. Oxidation of Polycyclic Aromatic Hydrocarbons under Sulfate-Reducing Conditions. *Appl. Environ. Microbiol.* **1996**, *62*, 1099–1101. [CrossRef] [PubMed]
97. Coates, J.D.; Woodward, J.; Allen, J.; Philp, P.; Lovley, D.R. Anaerobic degradation of polycyclic aromatic hydrocarbons and alkanes in petroleum-contaminated marine harbor sediments. *Appl. Environ. Microbiol.* **1997**, *63*, 3589–3593. [CrossRef] [PubMed]
98. Davidova, I.A.; Boris, W.; Callaghan, A.V.; Duncan, K.E.; Marks, C.R.; Suflita, J.M. *Dethiosulfatarculus sandiegensis*, sp. nov. gen. nov., isolated from a methanogenic paraffin-degrading enrichment culture and emended description of Desulfarculaceae Family. *Int. J. Syst. Evol. Microbiol.* **2016**, *66*, 1242–1248. [CrossRef]
99. Chen, J.; Liu, Y.F.; Zhou, L.; Mbadinga, S.M.; Yang, T.; Zhou, J.; Liu, J.F.; Yang, S.Z.; Gu, J.D.; Mu, B.Z. Methanogenic degradation of branched alkanes in enrichment cultures of production water from a high-temperature petroleum reservoir. *Appl. Microbiol. Biotechnol.* **2019**, *103*, 2391–2401. [CrossRef]
100. Mohamad Shahimin, M.F.; Foght, J.M.; Siddique, T. Methanogenic Biodegradation of iso-Alkanes by Indigenous Microbes from Two Different Oil Sands Tailings Ponds. *Microorganisms* **2021**, *9*, 1569. [CrossRef]
101. Martins, C.C.; de Abreu-Mota, M.A.; do Nascimento, M.G.; Dauner, A.L.L.; Lourenço, R.A.; Bícego, M.C.; Montone, R.C. Sources and depositional changes of aliphatic hydrocarbons recorded in sedimentary cores from Admiralty Bay, South Shetland Archipelago, Antarctica during last decades. *Sci. Total Environ.* **2021**, *795*, 148881. [CrossRef]
102. Avigan, J.; Blumer, M. On the origin of pristane in marine organisms. *J. Lipid Res.* **1968**, *9*, 350–352. [CrossRef] [PubMed]
103. Rocha, C.A.; Pedregosa, A.M.; Laborda, F. Biosurfactant-mediated biodegradation of straight and methyl-branched alkanes by *Pseudomonas aeruginosa* ATCC 55925. *AMB Express* **2011**, *1*, 9. [CrossRef] [PubMed]
104. Li, C.; Zhou, Z.X.; Jia, X.Q.; Chen, Y.; Liu, J.; Wen, J.P. Biodegradation of crude oil by a newly isolated strain *Rhodococcus* sp. JZX-01. *Appl. Biochem. Biotechnol* **2013**, *171*, 1715–1725. [CrossRef] [PubMed]
105. Cox, R.E.; Maxwell, J.R.; Myers, R.N. Monocarboxylic acids from oxidation of acyclic isoprenoid alkanes by *Mycobacterium fortuitum*. *Lipids* **1976**, *11*, 72–76. [CrossRef]
106. Dawson, K.; Schaperdoth, I.; Freeman, K.H.; Macalady, J.L. Anaerobic biodegradation of the isoprenoid biomarkers pristane and phytane. *Org. Geochem.* **2013**, *65*, 118–126. [CrossRef]
107. Caldwell, M.E.; Garrett, R.M.; Prince, R.C.; Suflita, J.M. Anaerobic biodegradation of long-chain n-alkanes under sulfate-reducing conditions. *Environ. Sci. Technol.* **1998**, *32*, 2191–2195. [CrossRef]
108. Hara, A.; Syutsubo, K.; Harayama, S. *Alcanivorax* which prevails in oil-contaminated seawater exhibits broad substrate specificity for alkane degradation. *Environ. Microbiol.* **2003**, *5*, 746–753. [CrossRef]
109. Gregson, B.H.; Metodieva, G.; Metodiev, M.V.; McKew, B.A. Differential protein expression during growth on linear versus branched alkanes in the obligate marine hydrocarbon-degrading bacterium *Alcanivorax borkumensis* SK2T. *Environ. Microbiol.* **2019**, *21*, 2347–2359. [CrossRef]